

# Calcareous nannofossils from the Eocene North Atlantic Ocean (IODP Expedition 342 Sites U1403–1411)

Paul R. Bown\*, Cherry Newsam

Department of Earth Sciences, University College London, Gower Street, London, WC1E 6BT, UK; \*p.bown@ucl.ac.uk

Manuscript received 23<sup>rd</sup> June, 2016; revised manuscript accepted 7<sup>th</sup> December, 2016

**Abstract** Integrated Ocean Drilling Program Expedition 342 (June–July 2012) cored nine sites and 18 holes (Sites U1403–U1411) on the J-Anomaly and the Southeast Newfoundland ridges in the NW Atlantic Ocean. These sites recovered sections ranging from Pleistocene to upper Albian, but the expedition particularly focussed on the recovery of expanded Paleogene successions with high quality microfossil preservation. This was achieved by choosing sites with thick packages of drift-type sediments on topographic highs that would maximise the preservation of carbonate. The expedition succeeded in recovering middle Eocene to lower Oligocene and upper Oligocene to lower Miocene high sedimentation rate sediment sequences with very well preserved microfossils. Highlights of the expedition include the recovery of continuous Eocene/Oligocene and Oligocene/Miocene boundaries, a Cretaceous/Paleogene boundary section with an intact spherule layer, and Cenomanian/Turonian section with a 44cm black shale. Here, we describe notable aspects of the Eocene nannofossil record, including the exceptional preservation and the evolution of several important Eocene groups: *Nannotetrina*, the *Sphenolithus furcatolithoides* group, the *Reticulofenestra bisecta* group and the *Coccolithus gigas* group. We also present a taxonomic overview of the Eocene nannofossil assemblages from Sites U1403–1411, illustrating 164 taxa and describing 25 new species (*Blackites friedrichii*, *Blackites sextonii*, *Blackites subtilis*, *Calcidiscus scullyae*, *Clausicoccus norrisii*, *Coccolithus hulliae*, *Coccolithus opdykei*, *Cruciplacolithus nishii*, *Helicosphaera prolixa*, *Holodiscolithus agninae*, *Holodiscolithus lippertii*, *Holodiscolithus liuii*, *Holodiscolithus whitesideae*, *Nannotetrina plana*, *Nannotetrina ruda*, *Neococcolithes purus*, *Neococcolithes radiatus*, *Pontosphaera brinkhuisii*, *Pontosphaera hollisii*, *Pontosphaera romansii*, *Pontosphaera wilsonii*, *Reticulofenestra magniscutum*, *Scyphosphaera interstincta*, *Semihololithus pseudobiskayae*, *Syracosphaera octiforma*) and five new combinations (*Blackites inversus*, *Pontosphaera zigzag*, *Reticulofenestra erbae*, *Reticulofenestra isabellae*, *Umbilicosphaera elliptica*).

**Keywords** Paleogene, Eocene, Oligocene, Atlantic, taxonomy, calcareous nannofossils

## 1. Introduction

Integrated Ocean Drilling Program Expedition (IODP Exp.) 342 (June–July 2012) cored nine sites and 18 holes (Sites U1403–U1411; Figure 1) on the J-Anomaly and Southeast Newfoundland ridges in the NW Atlantic Ocean, recovering a virtually complete composite section ranging from upper Albian to Pleistocene, representing 100Ma of Earth history (Figure 2). Moving downhole, the youngest 15 million year portion of this record (middle Miocene to Recent) is typically represented by thin Pleistocene foraminifer-rich sandy clay, and thin, stratigraphically-short, sections of Pliocene and upper Miocene clay, often with manganese nodules. Below the middle Miocene, the stratigraphic histories of the sites fall into two distinct groups, corresponding to the J-Anomaly ridge and SENR (Southeast Newfoundland ridge) locations.

The J-Anomaly sites typically comprise high sedimentation-rate lower Miocene to upper Oligocene sequences, with occasional minor hiatuses, and lower sedimentation-rate Oligocene to Paleocene sequences. The lower Eocene to Paleocene sequence is relatively condensed (Site U1406) and/or contains one or two minor

hiatuses (Site U1403 and U1406). Complete Miocene/Oligocene boundary sections were recovered at sites U1404 through U1406, and complete but lower sedimentation rate Oligocene/Eocene boundary sections at Site U1404 and U1406. Site U1403 is the deepest site on J-Anomaly ridge and recovered a lower Eocene through upper Cretaceous sequence, with several key intervals, including the early Eocene thermal maximum 2 (ETM 2), Paleocene-Eocene thermal maximum (PETM) and Cretaceous-Paleogene (K/Pg) boundary event (Figure 2).

The SENR sites comprise short Pleistocene and Neogene sequences overlying higher sedimentation-rate Oligocene through Paleocene sections. The highest sedimentation-rate, clay-rich drift sediments include middle Eocene sections at sites U1408 through U1410, and an upper Eocene through Oligocene section at Site U1411. These clay-rich sediments contain exceptionally well-preserved calcareous microfossils, including glassy planktic foraminifers and a diverse range of fragile and small nannoplankton. The carbonate-rich lower Eocene lithologies contain less well-preserved calcareous microfossils but nevertheless provide a relatively continuous stratigraphic record. PETM-equivalent sequences are present at

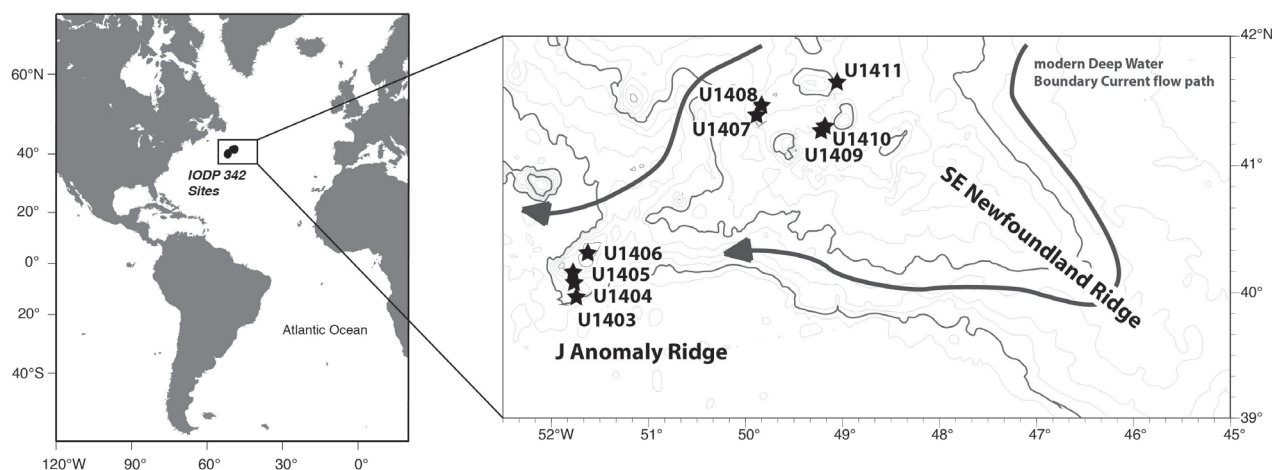


**Figure 1:** Location map of the sites drilled during IODP Expedition 342

sites U1407 and U1409, but the stratigraphy is condensed and/or includes minor hiatuses and, in the core of the event interval, the sediments are indurated, silicified and include chert beds. Site U1407 also recovered a long Cretaceous sedimentary record from the upper Maastrichtian to upper Albian, although a relatively large hiatus cuts out the lower Maastrichtian and upper Campanian. Sedimentation rates are low (0.15–0.41 cm/k.y.), but there is a relatively continuous record from the lower Campanian through upper Albian, including a striking Cenomanian/Turonian boundary black shale sequence representing OAE (Oceanic Anoxic Event) 2, and an Albian–Cenomanian section lying over shallow-water carbonate facies (Figure 2).

Initial biostratigraphic results are published in Norris *et al.* (2014), and high resolution integrated stratigraphic, isotopic and palaeoecological studies are in progress. In this paper, we describe some notable aspects of the Eocene nannofossil record, including the exceptional preservation and the evolution of several important Eocene groups: *Nannotetrina*, the *Sphenolithus furcatolithoides* group, the *Reticulofenestra bisecta* group and the *Coccolithus gigas* group. We also provide a taxonomic overview of the Eocene nannofossil assemblages from Sites U1407–1411, illustrating c. 150 taxa and including the description of 25 new species and five new combinations.

## 2. Material and methods

Nannofossils were viewed in simple smear-slides (Bown & Young, 1998), using transmitted-light microscopy (Zeiss Axiophot) in cross-polarised light (XPL) and phase contrast (PC) at  $\times 1000$ – $1600$ . Selected samples were also examined in the SEM (scanning electron microscope; JEOL Digital JSM-6480LV) in order to confirm the high quality preservation that is evident in the LM (light microscope). Here we report on the middle Eocene through lower Oligocene sections from Sites U1407–1411, which include the best preserved Paleogene nannoplankton.

## 3. Biostratigraphy

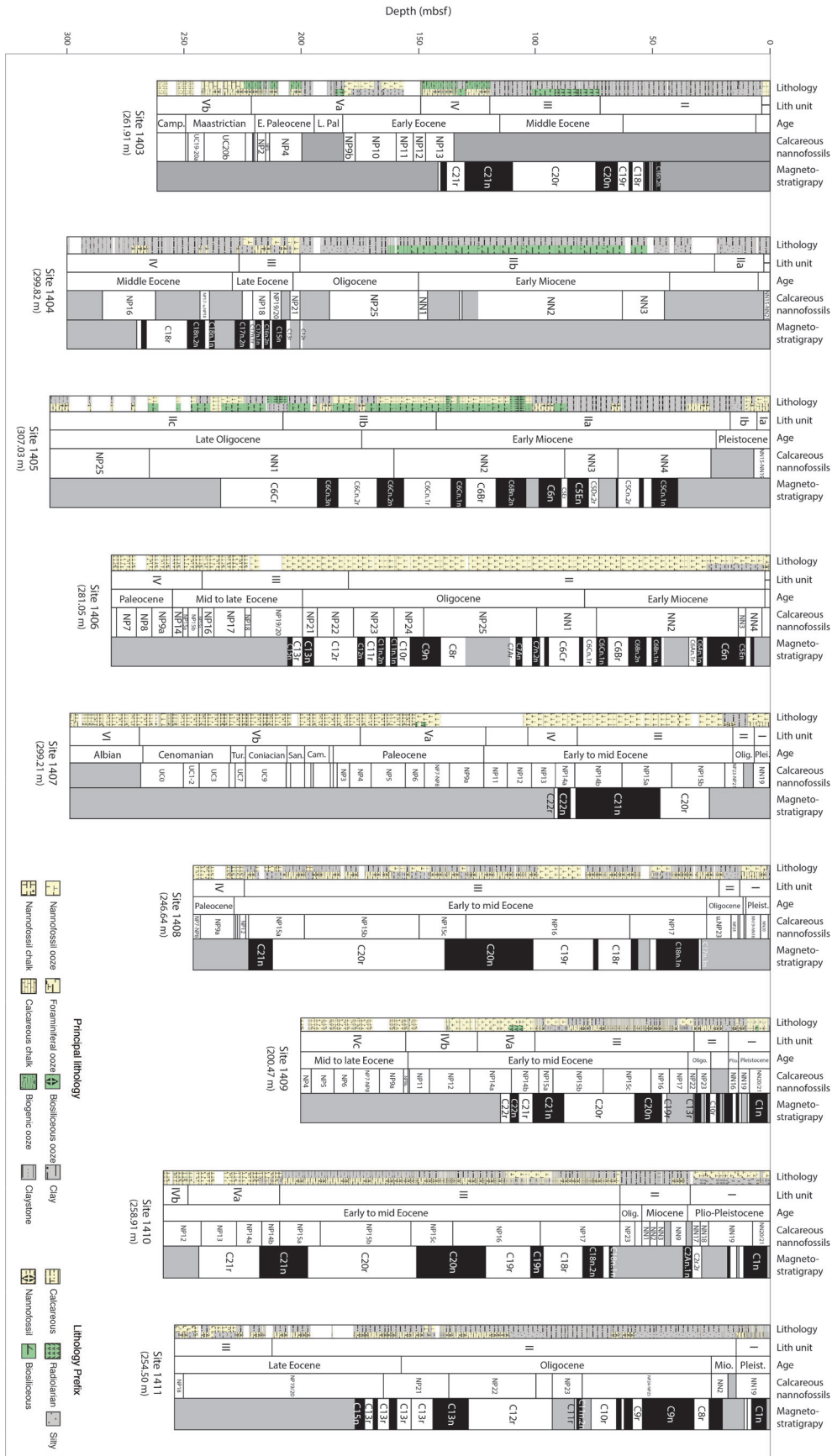
Semi-quantitative biostratigraphic data were generated during Exp. 342 and initial results are given in Norris *et al.* (2014), including range charts. In the Paleogene part of the section the nannofossil biozonation of Martini (1971) was used, and the Exp. 342 timescale, based on Gradstein *et al.* (2012), is applied herein (see Norris *et al.*, 2014, fig. F5).

## 4. Exceptional microfossil preservation in clay-rich drift sediments

One of the primary objectives of Exp. 342 was the recovery of high accumulation-rate, clay-rich sediments containing well-preserved microfossils suitable for geochemical and microfossil assemblage studies. Where drift sediments were recovered, we observed calcareous microfossil preservation that was good and moderate to good, and significantly better than the quality of preservation that is typical of most Paleogene deep-sea deposits. Furthermore, significant intervals of these drift successions contained exceptionally preserved calcareous microfossils, including diverse, minute and fragile calcareous nannofossils (see Plates 1–15 herein) and glassy planktic foraminifera (Norris *et al.*, 2014, Fig. F36). Such high quality preservation is usually only found in clay-rich, hemipelagic shelf successions, and the recovery of stratigraphically-continuous and expanded middle Eocene through lower Miocene successions with exceptional microfossil preservation was a significant success of the expedition.

## 5. Expedition 342 nannofossil occurrences: preservation or ecology?

The recent discovery of many new Paleogene taxa in the Tanzanian microfossil lagerstätte has led to re-evaluation of the taphonomic and ecological processes governing the preserved fossil record of calcareous nannoplankton (Bown *et al.*, 2008; Dunkley Jones *et al.*, 2009). The contrasting shelf and ocean distribution records of many nannofossil taxa, being rare or absent in deep-sea sediments

Figure 2: Summary of the stratigraphy recovered during IODP Expedition 342 (after Norris *et al.*, 2014)

and common and/or diverse in hemipelagic successions, can be interpreted as predominantly a taphonomic signal, an ecological signal, or some combination of both factors (Bown *et al.*, 2008). The Tanzanian lagerstätte is characterised by high abundances and/or diversity of Braarudosphaeraceae, Pontosphaeraceae, Rhabdosphaeraceae (especially *Blackites*), holococcoliths (e.g., *Clathrolithus*, *Holodiscolithus*, *Lanternithus*), and rarer occurrences of deep-time representatives of Calciosoleniaceae (*Calciosolenia*), Syracosphaeraceae (*Syracosphaera*) and abundant *Gladiolithus*. In addition, hemipelagic sediments tend to contain far greater numbers of very small ( $<3\mu\text{m}$ ) coccoliths, which are often numerically dominant (e.g., Gibbs *et al.*, 2006; Dunkley Jones *et al.*, 2009; Bown, 2016; this work). Disentangling which is the prevalent control on these distributions is difficult because the majority of deep-sea sediments are either carbonate-rich or have undergone dissolution, and are therefore rarely free from the overprint of strong diagenetic modification processes. The Exp. 342 sites provide new insight into this problem because the incorporation of a significant clay component has resulted in the accumulation of hemipelagic-like sediments with improved preservation potential but in a truly oceanic setting (3.0–4.0 km current depth; 2.6–3.1 km palaeo-depth at 50 Ma). Through much of the Paleogene and lower Neogene succession we are able to dismiss dissolution and overgrowth as a major factor controlling the presence or absence of nannofossils, and so the predominant factor on distribution is most likely the result of ecology. It should also be noted that there is little evidence of any significant microfossil reworking through these successions.

**Braarudosphaeraceae.** Braarudosphaeraceae is one group in which there is a relatively straightforward explanation for their strongly skewed shelf-sea distribution, because both extant and fossil forms are almost exclusively neritic, with rare oceanic occurrences explained by atypical events or environmental conditions (e.g. Kelly *et al.*, 2003). This is confirmed in the Exp. 342 sites, which are virtually devoid of braarudosphaerids, with the exception of:

1. a short mid-Cretaceous interval (Albian-Cenomanian) with *Braarudosphaera africana* at Site U1407 where shallow water, initially reefal, conditions occurred early in the site's history;
2. very rare occurrences of *Braarudosphaera bigelowii* in the post-K/Pg mass extinction recovery interval at Site U1403; and
3. a short interval, at the Oligocene/Miocene boundary of Site U1405, which represents a period of unusual conditions with common *Braarudosphaera* and *Micrantholithus* (see Norris *et al.* 2014 for further details).

**Holococcoliths.** In general, the Exp. 342 holococcoliths are not as common or diverse as seen in the Tanzanian succession (Plates 10, 15), suggesting environmental factors play a role in their oceanic distribution. In this case,

this may reflect the higher latitude position of the NW Atlantic area, or, alternatively, the outer shelf setting of Tanzania may have been richer in holococcoliths than the open-ocean. There are one or two exceptions to this, however, with *Zygrhablithus bijugatus* common through much of the Eocene succession, as it is in many other oceanic sites, confirming its widespread distribution in shelf and oceanic successions alike (Schneider *et al.*, 2011; Gibbs *et al.*, 2016). Also, *Daktylethra unitatis* is present through the Exp. 342 middle to upper Eocene, and ranges into the lower Miocene, extending the stratigraphic range of this taxon considerably. *Lanternithus minutus*, which is common in Tanzania, is only sporadically present at the Exp. 342 sites and never common.

**Rhabdosphaeraceae.** The occurrence of rhabdolites in the Exp. 342 material is comparable to the Tanzania succession, with several taxa common and consistently present, e.g. *Blackites amplus*, *B. tenuis*, *B. stilus* and *B. spinosus*. At least 12 of the 15 new rhabdolith taxa described from this stratigraphic interval in Tanzania (Bown, 2005; Bown & Dunkley Jones, 2006), are also present in the NW Atlantic (*B. bullatus*, *B. flammeus*, *B. furvus*, *B. fustis*, *B. globulus*, *R. gracilentus*, *B. kilwaensis*, *B. ornatus*, *B. rotundus*, *B. stilus*, *B. tortilis* and *B. virgatus*) and three more species are described herein (see below and Plates 8, 9, 15). This indicates that the rhabdolith group in general was broadly distributed in the Eocene with neritic and oceanic occurrences.

**Small coccoliths.** The link between preservation of small coccoliths and taphonomy is clearly demonstrated by comparison of modern taxa with the Holocene fossil record, which typically lacks coccoliths with length  $<3\mu\text{m}$  (Young *et al.*, 2005). When high quality nannofossil preservation is encountered in the fossil record then the presence of abundant, very small coccoliths is usually striking (Bown *et al.*, 2008). This is confirmed in the Exp. 342 material, in which small coccoliths ( $<3\mu\text{m}$ ) are dominant where preservation is good. In the middle Eocene to lower Oligocene interval, these coccoliths are predominantly reticulofenestrids, which typically make up ~50–60% of the assemblage (see, e.g., Plate 13, figs 1–6). Small representatives of coccolithaceans (e.g. *Coccolithus*, *Clausicoccus*) may also be common (Pl. 13, fig. 21; Pl. 14, fig. 9).

**Other taxa.** Other assemblage characteristics that are comparable with the Tanzania successions include high diversities in *Pontosphaera*, *Scyphosphaera* (Plates 6, 14) and *Helicosphaera* (Plates 5, 14) (six new species described herein), and the consistent occurrence of Eocene representatives of *Calcidiscus* and *Umbilicosphaera* (Plate 4, 5).

## 6. Evolution of the genus *Nannotetrina*

*Nannotetrina* is a short-lived, middle Eocene nannofossil genus comprising around six species that are typically large, three-dimensional nannoliths with square, cruciform

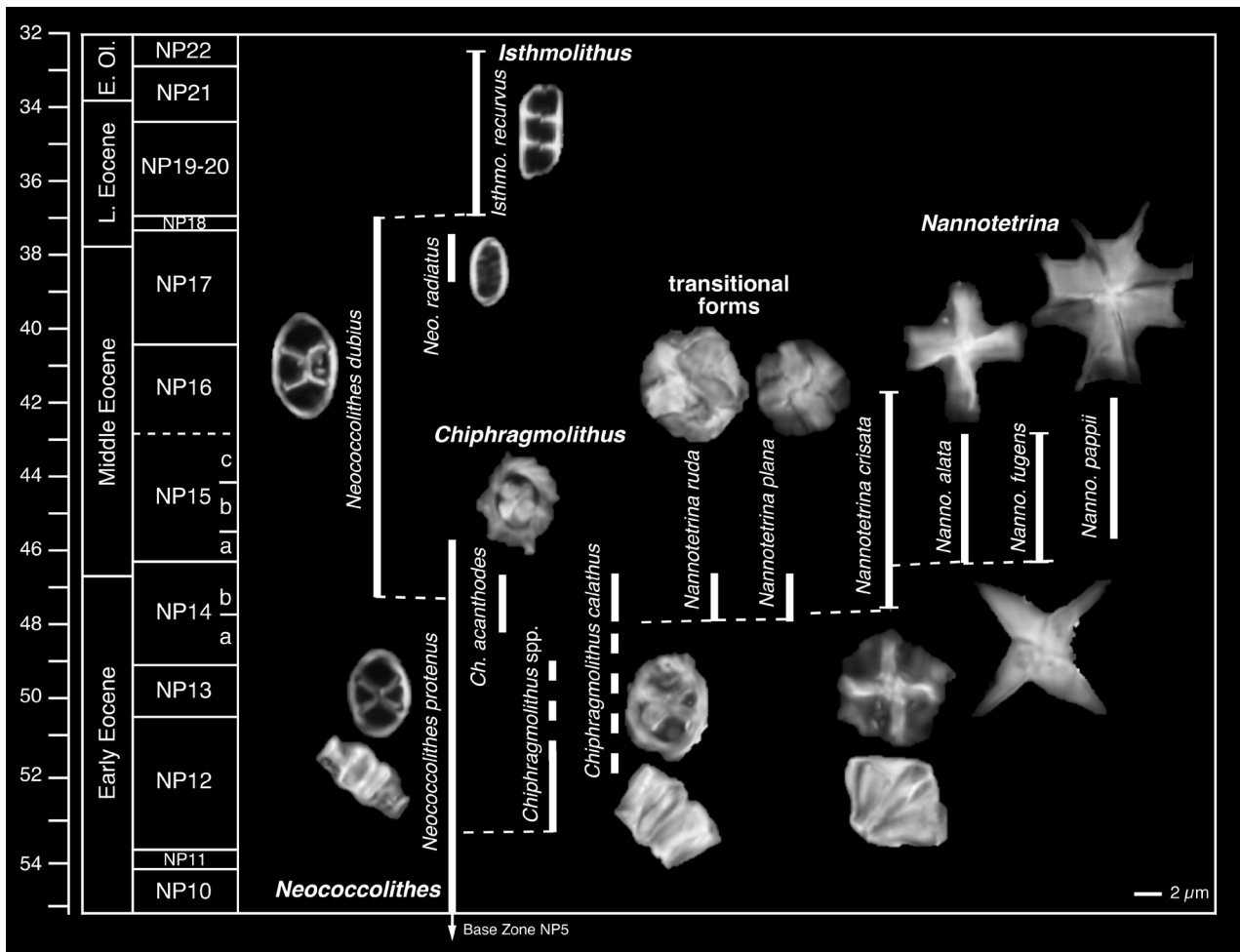


**Figure 3:** Stratigraphic distribution and possible phylogenetic relationships within *Nannotetrina* and related taxa. The timescale is from Norris *et al.* (2014). Dotted vertical lines are uncertain stratigraphic ranges, horizontal bars indicate well constrained range base or top

or stellate outlines and four diagnostic raised ridges or crossbars (see Figure 3 and Plate 7). In XPL the nannoliths are typically dark yellow to brown, indicating construction from few crystal units (at least four) that share high-angled c-axis crystallographic orientation, i.e., the elements are in extinction when lying flat. The unusual morphology of *Nannotetrina* has led to a number of different suggestions for their origin, ranging from nannolith ancestors, such as *Micula*, to more straightforward origins within Eocene coccolith groups, particularly from within the Zygodiscaceae. Several authors have discussed the Zygodiscaceae ancestry (Bramlette & Sullivan, 1961; Perch-Nielsen, 1985) and, specifically, that they originated as modified, enlarged central-area crossbar structures from which the coccolith rim has been lost. Thickened and elevated crossbars are seen in both *Neococcolithes* and *Chiphragmolithus* in the stratigraphic interval preceding the appearance of the first *Nannotetrina* in Zone NP14 and so there is good stratigraphic support for this hypothesis. *Nannotetrina* also have comparable crystallography to the crossbars of *Neococcolithes* and *Chiphragmolithus*, i.e., they

have high-angle c-axes. Unfortunately, the *Chiphragmolithus* group is poorly documented and stratigraphic ranges are not well constrained, but they are reported from Zone NP12 to NP14 (Bramlette & Sullivan, 1961; Shamrock & Watkins, 2012).

The link to the Cretaceous genus *Micula* was proposed by Romein (1979) and further discussed in Perch-Nielsen (1985) but there is little to support the idea as it is based on the erroneous observation that *Micula* ranged consistently through the Paleocene-Eocene, whereas these occurrences are now considered to be reworking. Further, the cubiform morphology of *Micula* is only very superficially similar to *Nannotetrina*, with *Micula* structure comprising far more numerous and complexly-intergrown crystal units with variable crystallographic orientations (see for example *Nannotax*: <http://www.mikrotax.org/Nannotax3/index.php?dir=Mesozoic/Nannoliths/Polycyclolithaceae/Micula>).

Expedition 342 nannofossil assemblages from Subzone NP14a include a range of morphotypes that appear to represent transitional forms between *Neococcolithes*/*Chiphragmolithus* and *Nannotetrina* (Figure 3 and

Plate 7). These assemblages include *Neococcolithes protenus* coccoliths with typical simple, narrow, mural rim and simple diagonal crossbars with all parts in near extinction in cross-polarized light (the R-unit proximal wall unit is very reduced in *Neococcolithes* and not visible in plan view in LM) (Pl. 7, figs 2–3). Alongside these forms are *Chiphragmolithus*-like coccoliths and *Nannotetrina*-like liths, which appear to represent transitional forms, as follows:

1. *Chiphragmolithus acanthodes* (Pl. 7, figs 4–12) – *Neococcolithes*-like but higher and larger with ragged outlines and crossbars that extend across the rim to the coccolith edge;
2. *Chiphragmolithus calathus* (Pl. 7, figs 13–15) – high and broadly-elliptical with high crossbars;
3. *Nannotetrina ruda* sp. nov. (Pl. 7, figs 16–20) – high, broad crossbars with reduced coccolith rim; and
4. *Nannotetrina plana* sp. nov. (Pl. 7, figs 21–30) – relatively flat with broad crossbars and a basal disc/rim.

This proliferation of morphologies occurs over a relatively short stratigraphic interval, immediately preceding the appearance of typical *Nannotetrina cristata* specimens (an elevated nannolith with four, relatively short crossbars/ridges that widen towards their ends and sit on a basal, plate-like structure: Pl. 7, figs 31–43), although several forms do continue alongside *Nannotetrina* through the upper part of Zone NP14. The transition from *Chiphragmolithus* to *Nannotetrina* thus appears to have been associated with a radiation in *Neococcolithes*/*Chiphragmolithus* coccoliths that include forms with *Nannotetrina* characters, such as reduction and loss of the mural rim, lateral and vertical expansion of the crossbars and formation of a basal structure. In some of the early *Nannotetrina* forms, multiple elements are evident in the basal disc in LM (e.g. Pl. 7, figs 31–36), but this is not obvious in the younger *Nannotetrina* specimens. The radiation also includes *Chiphragmalithus*-like coccoliths such as *C. acanthodes* that may be related to the *Chiphragmalithus* species described from the older Zone NP12 interval, but perhaps more likely represent homeomorphs within the *Neococcolithes* lineage. The disarticulated crossbars of *Chiphragmalithus*/*Neococcolithes* coccoliths are also documented from this stratigraphic interval (e.g. Bown & Dunkley Jones, 2012) and these may account for older records of small '*Nannotetrina*' (e.g., Bralower & Mutterlose, 1995).

After the appearance of *N. cristata* in Subzone NP14b a number of specimens were observed that show relict coccolith-rim and crossbar-like structures at the base of the larger cruciform nannolith (Pl. 7, figs 37–43, indicated by arrows on the images), providing further support for these nannoliths being highly modified coccoliths that have lost much of or their entire coccolith rim. In these specimens, the relict rims are far smaller in diameter than the main cross structure. In later species of *Nannotetrina*, e.g., *N. fulgens*, the crossbars become

very long and form free-rays with reduced basal structure or inter-arm fill (Pl. 12, fig. 12). In other species, such as *N. spinosa* and *N. pappii*, additional ridges become prominent giving the nannoliths a stellate appearance (Pl. 7, fig. 44).

## 7. Evolution of large middle Eocene Coccolithaceae

The middle Eocene is characterized by the occurrence of particularly large (>12µm) coccolithacean coccoliths (see examples shown in Plates 3 and 12), which have been included in a number of different genera including *Coccolithus*, *Chiasmolithus*, *Cruciplacolithus* and *Birkelundia*. The generic assignment has been particularly influenced by the relative importance placed upon central area structures, although modern representative of *Coccolithus* may develop both transverse and axial crossbars. The middle Eocene forms with wide central areas, relatively narrow tube cycles and diagonal crossbars are clearly correctly grouped within *Chiasmolithus* (e.g. *C. grandis*, *C. expansus*: Pl. 3, figs 27–29; Pl. 12, fig. 4) but the generic affinity of other species is less clear cut. One group most-closely resembles *Coccolithus*, with relatively narrow central-areas and broad tube-cycles but they have crossbars, usually axial, more rarely rotated. Although these taxa have sometimes been included within *Cruciplacolithus*, they are now more frequently classified as *Coccolithus* (e.g. *Coccolithus mutatus*, *Coccolithus staurion*). The distinctive marker species, '*Chiasmolithus*' *gigas* also appears to be one of these forms (original described as *Coccolithus*, but subsequently reassigned based on the presence of diagonal crossbars) and this is supported by new observations from the Exp. 342 material (Plate 3). These reveal a range of morphologies, comprising a lineage with early forms having broad, axial crossbars (assigned to *C. staurion* herein: Pl. 3, figs 5–11) that give rise to coccoliths with rotated, asymmetric crossbars (named *C. cf. C. gigas* herein: Pl. 3, figs 12–20, 23–24) and then to forms with diagonal crossbars that characterise *C. gigas* (Pl. 3, figs 21–22, 25–26). The very large forms with axial and asymmetric crossbars first appear near the Zone NP14–15 boundary, preceding the appearance of *C. gigas sensu stricto*, which marks the base of Subzone NP15b. This lineage strongly suggests that the '*Chiasmolithus*' genus, as currently used, is polyphyletic and the species *gigas* is reinstated to its original genus, *Coccolithus*, herein.

In addition to these very large forms, the middle Eocene assemblages also contain a diverse range of large *Coccolithus* coccoliths, including forms with crossbars (*C. hulliae* sp. nov., *C. opdykei* sp. nov.) and transverse bars (*C. bipartoperculatus*).

## 8. Evolution of the *Sphenolithus furcatolithoides* group

*Sphenolithus furcatolithoides* are highly distinctive middle Eocene sphenoliths (Zones NP15b–NP16), with spines

that bifurcate but remain roughly parallel before diverging again high-up on the spine (Plate 11). Shamrock (2010) showed that this highly distinctive species was preceded by forms with spines that diverge at a higher angle, low on the spine, calling the species *S. perpendicularis*. The excellent preservation of the Exp. 342 material reveals a wide range of different morphotypes within this group, including early spinose forms with very high-angle narrow spines (*S. cf. S. perpendicularis* herein; Pl. 11, figs 1–3), a variety of *S. perpendicularis* types (Pl. 11, figs 7–13), and *S. furcatolithoides* variants with spines that converge or diverge at different angles high-up along the spine (Pl. 11, figs 15–22, 26). These spines can be extremely long, up to 25 µm in length, and represent some of the ‘largest’ nannofossils ever found. The morphology of specimens close to the first appearance of *S. furcatolithoides* itself suggest that it may have evolved from a *S. radians*-like ancestor, rather than the preceding widely-bifurcating forms (Pl. 11, fig. 14).

### 9. Evolution of the *Reticulofenestra bisecta* group

Reticulofenestrid coccoliths with closed central areas are known through most of this group's history (lower Eocene to Recent), but the appearance of common, medium- to large-sized forms with conspicuous (birefringent), distal central-area ‘plugs’ (the *R. bisecta* group of Bown & Dunkley Jones, 2012; Pl. 2, figs 20–44) is a highly distinctive stratigraphic signal occurring in lowermost Zone NP17 (~40.36 Ma) and close to the onset of the Middle Eocene climatic optimum (MECO) event (Fornaciari *et al.*, 2010). However, the discovery of very rare and unusual *R. bisecta*-like coccoliths in Subzone NP15 (from ~46 Ma) in the Exp. 342 material indicates that the group had a cryptic origination at least six million years earlier than this (Pl. 2, figs 25–44). These coccoliths, named *R. magniscutum* sp. nov. herein, have very unusual, thickened, dome-like distal shields but possess the distinctive central plug that is characteristic of the *R. bisecta* group.

It should be noted that this distinctive reticulofenestrid group includes *R. stavensis* (>10 µm) and *R. bisecta* (<10 µm) but that these species are also placed in a separate genus, *Dictyococcites*, by some authors, and different species names, e.g. *hesslandii* and *scrippsae*, and size categories are also applied (e.g. Agnini *et al.*, 2014). In addition, reticulofenestrids with simple, closed central areas are also referred to as *R./D. bisecta* by some authors, but we consider these to be separate taxa, though poorly defined in current classifications (see below for further discussion).

## 10. Systematic palaeontology

This section provides images of a representative selection of nannofossils from the IODP Exp. 342 Eocene sites (U1403–1411) in 12 LM plates and three SEM plates (Plates 13–15). The LM images are reproduced at constant

magnification, and a 2 µm scale bar is provided beside at least one of the images on each plate. Taxonomic comments are only provided for notable taxa and the description of 25 new species. The taxonomic listing refers only to species illustrated in the plates. Sample information is provided using standard IODP notation (Hole-Core-Section, depth in cm in section). The descriptive terminology (including size classes) follows the guidelines of Young *et al.* (1997). The higher taxonomy follows the scheme for extant coccolithophores of Young *et al.* (2003) and, for the extinct taxa, the scheme of Young & Bown (1997) and *Nannotax* (<http://www.mikrotax.org/Nannotax3>). All new taxonomic names are Latin, unless stated otherwise, and the meaning is given in each case. Range information is given for stratigraphic distributions in the Exp. 342 sites, unless stated otherwise. Only bibliographic references not included in Perch-Nielsen (1985), Bown (1998) or Jordan *et al.* (2004) are included in the reference list. A comprehensive list of bibliographic references can also be found on *Nannotax*. The following abbreviations are used: LM – light microscope, XPL cross-polarised light, PC – phase-contrast illumination, L – length, H – height, W – width, D – diameter. Type material and images are stored in the Department of Earth Sciences, University College London.

### 10.1 Placolith coccoliths

#### Order ISOCHRYSIDALES Pascher, 1910

Family NOELAERHABDACEAE Jerkovic, 1970  
emend. Young & Bown, 1997

#### *Cyclicargolithus floridanus* Group

Pl. 1, figs 20–27; Pl. 13, fig. 7

**Description:** Subcircular to broadly elliptical reticulofenestrids with narrow central area and thin, imperceptible net (non-birefringent or lost).

*Cyclicargolithus* cf. *C. abisectus* (Müller, 1970) Wise,  
1973

Pl. 1, fig. 25

**Remarks:** Used here for rare, but conspicuous, very large, subcircular reticulofenestrids seen in the middle Eocene (e.g. Zone NP14) and similar in overall morphology to the younger, Oligocene, species *C. abisectus*.

*Cyclicargolithus floridanus* (Roth & Hay, in Hay *et al.*,  
1967) Bukry, 1971

Pl. 1, figs 20–24; Pl. 13, fig. 7

**Remarks:** Used in a broad sense here for subcircular reticulofenestrids with narrow central area. Specimens with closed central areas are called *Cyclicargolithus* cf. *C. floridanus*.

*Cyclicargolithus* cf. *C. floridanus* (Roth & Hay, in Hay  
*et al.*, 1967) Bukry, 1971

Pl. 1, figs 26–27

**Remarks:** Like *C. floridanus* but with closed central area.

*Cyclicargolithus luminis* (Sullivan 1965) Bukry 1971  
sensu Shamrock & Watkins, 2012  
Pl. 1, figs 28–29

**Remarks:** A distinctive, birefringent circular coccolith occurring rarely in Zone NP14 to Subzone NP15a at Sites U1407–1410. It is distinguished by relatively straight and axial extinction lines. Shamrock & Watkins (2012) discuss the differentiation between this and the older *Cyclicargolithus parvus* Shamrock & Watkins, 2012 species (previously called *C. luminis* in Bown, 2005).

#### *Reticulofenestra bisecta* Group

Pl. 2, figs 20–44; Pl. 13, fig. 11

**Description:** Elliptical reticulofenestrids with central area closed by a robust, conspicuous distal ‘plug’ (birefringent). In the type upper Eocene specimens this plug is a distal structure that is underlain by a proximal coarse grill of near radial laths. Thus defined, the stratigraphic range of the group is middle Eocene to lowermost Miocene. We do not include reticulofenestrid coccoliths in which the central area is simply closed (e.g. see Pl. 1, figs 26–27; Pl. 2, figs 17–19, 24), although these taxa are poorly served by current reticulofenestrid nomenclature. Some authors consider these forms to be ecophenotypic variants (e.g., Young, 1990, 1998), while others apply a parallel taxonomy or broaden the taxonomic concept of taxa such as *bisecta*. **Included species:** *R. bisecta*, *R. filewiczii*, *R. magniscutum*, *R. stavensis*.

*Reticulofenestra bisecta* (Hay *et al.*, 1966) Roth, 1970  
Pl. 2, figs 20–21; Pl. 13, fig. 11

**Remarks:** Less than 10  $\mu\text{m}$  in length (the holotype is 8  $\mu\text{m}$ ).

*Reticulofenestra filewiczii* (Wise & Wiegand *in* Wise,  
1983) Dunkley Jones *et al.*, 2009  
Pl. 2, fig. 23

**Remarks:** Appears at the same time as other members of the *R. bisecta* group and is probably closely related to these forms, differing only in having a small central opening.

*Reticulofenestra magniscutum* sp. nov.

Pl. 2, figs 25–44

**Derivation of name:** From *magnus*, meaning ‘elevated’, and ‘*scutum*’ meaning shield, referring to the elevated distal shield of this species. **Diagnosis:** Large, elliptical reticulofenestrids with a thickened, dome-like distal shield and central area filled with a plug. **Differentiation:** Similar to other species of the *Reticulofenestra bisecta* group but with an elevated, dome-like distal shield, which is therefore highly birefringent (orange) in XPL and frequently seen in side view (Pl. 2, figs 41–44).

**Remarks:** We have observed this species from a short stratigraphic interval in the middle Eocene (Subzone NP15a–lower Zone NP16), in an interval that predates the common occurrence of other members of the

*Reticulofenestra bisecta* group by around 6 m.y. The species is very rare and so tracing the relationship between *R. magniscutum* and *R. bisecta* has not been possible.

**Dimensions:** Holotype L = 8.5  $\mu\text{m}$  (Paratype L = 9.0  $\mu\text{m}$ ). Side view coccolith height ~6.5  $\mu\text{m}$ . **Holotype:** Pl. 2, figs 25–28. **Paratype:** Pl. 2, figs 31–36. **Type locality:** IODP Hole U1408A, NW Atlantic Ocean. **Type level:** Middle Eocene, Sample U1408A-14X-5, 63cm (Zone NP16). **Occurrence:** Rare. Subzone NP15a–Zone NP16; IODP Sites U1408, U1409 and U1410.

*Reticulofenestra stavensis* (Levin & Joerger, 1967)  
Varol, 1989

Pl. 2, fig. 22

**Remarks:** Greater than 10  $\mu\text{m}$  in length (the holotype is 14  $\mu\text{m}$ ).

#### *Reticulofenestra reticulata* Group

Pl. 2, figs 3–16; Pl. 13, figs 12–16

**Remarks:** Typically circular reticulofenestrids with circular central area spanned by robust, visible net (birefringent). We currently include *R. erbae* (closed central-area), *R. isabellae* (>12  $\mu\text{m}$ , broad tube-cycle and narrow central-area); *R. reticulata* (<12  $\mu\text{m}$ , broad tube-cycle and narrow central-area) and *R. westerholdii* (medium-sized with less conspicuous tube cycle and inconspicuous or no central net).

*Reticulofenestra erbae* Fornaciari *et al.*, 2010 comb.  
nov.

Pl. 2, figs 13–14; Pl. 13, fig. 12

**Basionym:** *Cribrocentrum erbae* Fornaciari *et al.*, 2010, p. 251, pl. 2, fig. 1, *Stratigraphy*, 7: 229–264.

*Reticulofenestra isabellae* Catanzariti *et al. in*  
Fornaciari *et al.*, 2010 comb. nov.

Pl. 2, figs 11–12; Pl. 13, fig. 16

**Basionym:** *Cribrocentrum isabellae* Catanzariti, Rio & Fornaciari *in* Fornaciari *et al.*, 2010, p. 252, pl. 2, fig. 4, *Stratigraphy*, 7: 229–264.

*Reticulofenestra reticulata* (Gartner & Smith, 1967)  
Roth & Thierstein, 1972

Pl. 2, figs 7–10; Pl. 13, figs 13–15

**Remarks:** Used in a broad sense here for circular reticulofenestrids with moderately-wide to narrow central areas and a visible net (birefringent). Very large forms (>12  $\mu\text{m}$ ) have been differentiated as *R. isabellae* (Pl. 2, figs 11–12) by Fornaciari *et al.* (2010) and we informally differentiated forms with wide central areas (Pl. 2, figs 7–9) and specimens with subcircular to elliptical outlines (Pl. 2, figs 3–6). Further subdivision may be warranted.

*Reticulofenestra westerholdii* Bown & Dunkley Jones,  
2012

Pl. 2, figs 15–16

**Remarks:** This species has an inconspicuous or no central net but is circular and is, in other respects, very similar to other species in the *R. reticulata* group.

***Reticulofenestra lockeri* Group**

Pl. 1, figs 30–43; Pl. 2, figs 1–2; Pl. 13, fig. 10

**Description:** Elliptical reticulofenestrids with relatively open central area and robust, visible net (birefringent).

*Reticulofenestra daviesii* (Haq 1968) Haq, 1971

Pl. 1, figs 33–36

**Remarks:** Differentiated from *R. lockeri* by a row of visible pores around the edge of the central net. Although this species becomes conspicuous and abundant around the Eocene/Oligocene boundary, it ranges down into the middle Eocene (Zone NP14) in the Exp. 342 material. **Occurrence:** Zone NP14–NP23.

*Reticulofenestra lockeri* Müller, 1970

Pl. 1, fig. 32; Pl. 13, fig. 10

**Occurrence:** Lower Eocene–lower Miocene (Zone NP13–NN2).

*Reticulofenestra* cf. *R. lockeri* Müller, 1970

Pl. 1, figs 30–31; Pl. 2, figs 1–2

**Remarks:** Indeterminate forms with central areas that are either narrower (Pl. 1, figs 30–31) or wider (Pl. 2, figs 1–2) than the typical morphology.

*Reticulofenestra macmillanii* Dunkley Jones *et al.*, 2009

Pl. 1, fig. 37

*Reticulofenestra onusta* (Perch-Nielsen, 1971) Wise, 1983

Pl. 1, figs 38–43

**Description:** Large to very large, distinctive elliptical reticulofenestrids with a wide central area spanned by a finely perforate, weakly birefringent net. **Differentiation:** Distinguished from other *R. lockeri* group coccoliths by large size, wider central area and clearly visibly fine perforations across the net. **Dimensions:** L = ~11.0–12.5 µm. **Occurrence:** Rare, but apparently restricted to Subzones NP15b–c; IODP Sites U1409, U1410. Holotype from Zone NP15. Questionable occurrences in Zone NP16 at Site U1410.

***Reticulofenestra umbilicus* Group**

Pl. 1, figs 8–19, 44–48; Pl. 12, figs 1–3;

Pl. 13, figs 8–9

**Description:** Elliptical reticulofenestrids with relatively open central area and thin, imperceptible net (non-birefringent or lost).

*Reticulofenestra dictyoda* (Deflandre in Deflandre & Fert, 1954) Stradner in Stradner & Edwards, 1968

Pl. 1, figs 9–12; Pl. 13, fig. 8

**Remarks:** Used here in a broad sense for elliptical reticulofenestrids with elliptical and relatively open central areas.

*Reticulofenestra hillae* Bukry & Percival, 1971

Pl. 1, figs 44–45

*Reticulofenestra minuta* Roth, 1970

Pl. 1, fig. 8; Pl. 13, figs 1–4

**Remarks:** Used here in a broad sense for very small (<3 µm), elliptical reticulofenestrids. Although they typically have open central areas, in SEM many specimens are seen with closed central areas and at this size it may be difficult to distinguish the different varieties in LM. Our SEM observations suggest there is considerable diversity of form in this size range.

*Reticulofenestra umbilicus* (Levin, 1965) Martini & Ritzkowski, 1968

Pl. 1, figs 46–48; Pl. 12, figs 1–3; Pl. 13, fig. 9

**Remarks:** The first appearance of very large, >14 µm, elliptical reticulofenestrids (the species *R. umbilicus*) has long been used as a distinctive stratigraphic marker (e.g. Backman & Hermelin, 1986). In the Exp. 342 material these sizes are attained by subcircular to elliptical reticulofenestrids (similar to *R. wadeae* and *R. umbilicus*) in Subzone NP15b, around 3 m.y. prior to the level typically cited for this biohorizon. Agnini *et al.* (2014) suggest that the use of the first common occurrence of *R. umbilicus* may represent a more consistent horizon, above the last occurrence of *C. gigas*.

*Reticulofenestra wadeae* Bown, 2005

Pl. 1, figs 13–19

Family **PRINSIACEAE** Hay & Mohler, 1967 emend.

Young & Bown, 1997

*Girgisia* Varol, 1989

*Girgisia gammation* (Bramlette & Sullivan, 1961)

Varol, 1989

Pl. 1, figs 5–7

Genus *Towieus* Hay & Mohler, 1967

Pl. 1, figs 1–4

**Remarks:** *Towieus* was one of the dominant placolith groups of the late Paleocene to early Eocene but declined, broadly coincident with the appearance and rise of the reticulofenestrid group in the early Eocene (zones NP12–13) (e.g., Agnini *et al.* 2006). The extinction of *Towieus* has remained poorly constrained with reports ranging from Zone NP12 (Bralower & Mutterlose 1995) to Zone NP15 (Perch-Nielsen, 1985). Relatively common *Towieus* coccoliths were documented in equatorial Pacific sites up to Zone NP15 by Bown & Dunkley Jones (2012) and similarly we see *Towieus* through to Subzone NP15b in the Exp. 342 sites (e.g. Site U1409), confirming this later extinction level.

*Toweius magnicrassus* Bukry, 1971

Pl. 1, figs 3–4

*Toweius pertusus* (Sullivan, 1965) Romein, 1979

Pl. 1, fig. 1

*Toweius patellus* Bown, 2016

Pl. 1, fig. 2

**Order COCCOLITHALES Haeckel, 1894 emend.  
Young & Bown, 1997**

Family **COCCOLITHACEAE** Poche, 1913 emend.  
Young & Bown, 1997

*Coccolithus biparteperculatus* (Varol, 1991) Bown &  
Dunkley Jones, 2012 Pl. 3, figs 30–31

*Coccolithus crassus* Bramlette & Sullivan, 1961

Pl. 2, figs 45–48

**Remarks:** Like *C. pelagicus* but with an unusually birefringent shield image in XPL. **Occurrence:** upper Zone NP12–14a (Wei, 1993).

*Coccolithus eopelagicus* (Bramlette & Riedel, 1954)

Bramlette & Sullivan, 1961

Pl. 12, fig. 5

*Coccolithus formosus* (Kamptner, 1963) Wise 1973

Pl. 13, figs 19–20

*Coccolithus hulliae* sp. nov.

Pl. 4, figs 7–17

**Derivation of name:** Named after Celli Hull (University of Yale, USA), Exp. 342 shipboard scientist, micropalaeontologist and palaeoceanographer. **Diagnosis:** Broadly elliptical coccolith with *Ericsonia*-like shield image and moderately wide central area (similar to shield width), spanned by conspicuous axial crossbars. **Remarks:** In XPL the shields appear similar to *Ericsonia* (i.e. with broad, bright tube cycle). Although *Ericsonia* coccoliths are rarely and sporadically seen through the Eocene, these are usually small, circular forms and we consider it most likely that this species arose from a *Coccolithus* ancestor. *Coccolithus hulliae* appears to be stratigraphically restricted to Zones NP14–15 in the Exp. 342 material. This species may have been identified as *Ericsonia insolita* Perch-Nielsen, 1971 in Bralower & Mutterlose (1995) and documented as having a first appearance in Subzone NP14a. **Differentiation:** Distinguished from other *Coccolithus* and *Ericsonia* by its distinctive shield image in XPL and moderately wide central area with conspicuous axial crossbars. **Dimensions:** Holotype L = 8.4 µm (Paratype L = 8.6 µm). **Holotype:** Pl. 4, figs 16–17. **Paratype:** Pl. 4, figs 13–15. **Type locality:** IODP Hole U1407A, NW Atlantic Ocean. **Type level:** Middle Eocene, Sample U1407B-8-CC (Subzone NP14b). **Occurrence:** Subzone NP14b–15b; IODP Sites U1407, U1408 and U1409. Site U865, Pacific Ocean (Bralower & Mutterlose, 1995).

*Coccolithus* cf. *C. hulliae* sp. nov. var. 1

Pl. 4, figs 1–4

**Remarks:** Similar to *C. hulliae* but with a transverse bar. **Occurrence:** Subzone NP14b–15b; IODP Sites U1407 and U1409.

*Coccolithus* cf. *C. hulliae* sp. nov. var. 2

Pl. 4, figs 5–6

**Remarks:** Similar to *C. hulliae* but with a moderately wide, apparently vacant, central area (similar to shield width). **Occurrence:** Subzones NP15b–c; IODP Site U1408.

*Coccolithus pauxillus* Bown, 2010 Pl. 4, figs 29–30;

Pl. 13, fig. 21

*Coccolithus pelagicus* (Wallich, 1877) Schiller, 1930

Pl. 13, figs 17–18

***Coccolithus gigas* Group**

Pl. 3, figs 1–26; Pl. 12, fig. 7

**Description:** Large to very large *Coccolithus* coccoliths with narrow to moderately-wide central areas spanned by crossbars that are conspicuous in light microscope.

**Remarks:** These coccoliths have previously been variously classified within the genera *Crucioplacolithus*, *Chiasmolithus* and *Coccolithus* but appear to represent a coherent lineage with stratigraphic range restricted to the mid-part of the Eocene (Zones 14–16). The inclusion of these species within the genus *Coccolithus* is consistent with the extant *Coccolithus* species, which can also produce central area bars and crosses. **Included species:** *C. gigas*, *C. mutatus*, *C. opdykei*, *C. staurion*.

*Coccolithus opdykei* sp. nov.

Pl. 3, figs 1–4

**Derivation of name:** Named after Bradley Opdyke (The Australian National University, Australia), Exp. 342 shipboard scientist and palaeoceanographer. **Diagnosis:** Large (<12 µm) *Coccolithus* with a narrow central area (<shield width) spanned by a broad, birefringent, axial to near-axial crossbars that nearly fill the central area. **Differentiation:** Smaller than *C. mutatus*, *C. staurion* and *C. cf. C. gigas*, with broader crossbars than *C. mutatus* and *C. staurion*. Similar to *Crucioplacolithus opacus* Shamrock & Watkins, 2012 but with a broader and brighter tube cycle in XPL. **Dimensions:** Holotype L = 11.1 µm (Paratype L = 9.6 µm). **Holotype:** Pl. 3, figs 2–3. **Paratype:** Pl. 3, fig. 1. **Type locality:** IODP Hole U1407A, NW Atlantic Ocean. **Type level:** Middle Eocene, Sample U1407A-8H-CC (Subzone NP14b). **Occurrence:** Subzones NP14b–15b; IODP Sites U1407 and U1409.

*Coccolithus gigas* Bramlette & Sullivan, 1961 emend.

Pl. 3, figs 21–22, 25–26; Pl. 12, fig. 7

**Emended diagnosis:** Very large *Coccolithus* with narrow to moderately wide central area spanned by thick crossbars which are diagonal or near diagonal in orientation, making an angle of 30° or greater with the longitudinal axis. **Differentiation:** Distinguished from *Coccolithus* cf.

*C. gigas* by bar angles that are rotated greater than 30° from the longitudinal axis. Typically the longitudinal bar is closer to axial than diagonal in *Coccolithus* cf. *C. gigas*. **Occurrence:** Subzone 15b.

*Coccolithus* cf. *C. gigas* Bramlette & Sullivan, 1961  
Pl. 3, figs 12, 15–17, 19–20, 23–24

**Description:** Very large *Coccolithus* with narrow to moderately wide central area spanned by thick crossbars which are rotated from axial by up to 29°. **Differentiation:** Distinguished from *C. gigas* by having near-axial to slightly rotated crossbars rather than diagonal or near-diagonal orientation, and from *C. mutatus* by the thicker crossbars. **Occurrence:** Subzones NP15a–b (rare, questionable specimens in NP14b and NP15c); IODP Sites U1407, U1408, U1409 and U14010.

*Coccolithus mutatus* (Perch-Nielsen, 1971) Bown, 2005  
Pl. 3, figs 7, 13–14, 18

**Description:** Very large *Coccolithus* with moderately-broad central area spanned by narrow crossbars that are axial or near axial. **Occurrence:** Zone NP14b–16; Sites U1407–U1410.

*Coccolithus staurion* Bramlette & Sullivan, 1961  
Pl. 3, figs 5–6, 8–11

**Description:** Very large (>12µm) *Coccolithus* with narrow central area spanned by robust axial crossbars. **Remarks:** The paratype has narrow bars and is probably a *C. mutatus* specimen. The holotype is large in size (12–15µm) and we distinguish smaller forms as *Coccolithus opdykei* sp. nov.. **Synonym:** *Coccolithus insolitus* (Perch-Nielsen, 1971) Ladner & Wise, 2002. **Occurrence:** Zone NP13–17; Sites U1407–U1410.

#### ***Chiasmolithus-Cruciplacolithus* Group**

*Bramletteius serraculoides* Gartner, 1969  
Pl. 4, figs 18–20

*Chiasmolithus expansus* (Bramlette & Sullivan, 1961)  
Gartner, 1970

Pl. 3, figs 27–29

*Chiasmolithus grandis* (Bramlette & Riedel, 1954)  
Radomski, 1968

Pl. 12, fig. 4

*Cruciplacolithus cruciformis* (Hay & Towe, 1962)  
Roth, 1970

Pl. 4, fig. 21

*Cruciplacolithus nishii* sp. nov.  
Pl. 4, figs 22–28

**Derivation of name:** Named after Hiroshi Nishi (Tohoku University, Sendai, Japan), Exp. 342 shipboard scientist and micropalaeontologist. **Diagnosis:** Medium sized *Cruciplacolithus* with narrow shields and wide central area spanned by narrow axial crossbars bearing a spine. **Differentiation:** Distinguished from other *Cruciplacolithus* by the wide central area and spine-bearing cross – an unusual

feature amongst Cenozoic placoliths. **Dimensions:** Holotype L = 4.2µm (Paratype L = 4.3µm). **Holotype:** Pl.4, fig. 27. **Paratype:** Pl.4, figs 24–26. **Type locality:** IODP Hole U1408A, NW Atlantic Ocean. **Type level:** Middle Eocene, Sample U1408A-4H-CC (Zone NP16). **Occurrence:** Zone upper NP16–17; IODP Site U1408, U1409.

#### ***Clausicoccus* Group**

Pl. 4, figs 33–45; Pl. 14, figs 9–13

**Remarks:** A wide range of sizes are seen in this group from very small (<3µm, e.g. *Clausicoccus* sp. small, Pl. 14, fig. 9) to very large (>12µm, e.g. *Clausicoccus vanheckiae* and *C. norrisii*, Pl. 4, figs 38–43), but all are characterised by coccolithacean-type rims with narrow to relict distal tube cycles and a relatively coarsely-perforate central area net. A number of SEMs suggests there is also a more finely perforate grill on the proximal side (Pl. 14, fig. 13).

*Clausicoccus fenestratus* (Deflandre & Fert, 1954)  
Prins 1979

Pl. 4, figs 35–36; Pl. 14, fig. 13

*Clausicoccus fenestratus* large (Deflandre & Fert, 1954) Prins 1979  
Pl. 4, fig. 37

**Remarks:** Like *C. fenestratus* but large (~9µm). Similar in size to *Clausicoccus vanheckiae* but with relatively broader rim and narrower central area with fewer perforations. These forms become conspicuous for a short stratigraphic interval in Zone NP17 in the Exp. 342 material.

*Clausicoccus* cf. *C. fenestratus* (Deflandre & Fert, 1954) Prins 1979  
Pl. 4, figs 44–45

**Remarks:** Like *Clausicoccus fenestratus* but the central, perforate plate takes the form of broad axial crossbars.

*Clausicoccus norrisii* sp. nov.  
Pl. 4, figs 40–43

**Derivation of name:** Named after Richard Norris (Scripps Oceanographic Institute, USA), Exp. 342 co-chief scientist, micropalaeontologist and palaeoceanographer. **Diagnosis:** Large, broadly elliptical coccolithacean coccolith with broad shields and moderately wide central area (similar to shield width) spanned by a plate that is indistinctly perforate and crossed by strong diagonal extinction lines. The bright inner cycle is relatively indistinct. **Remarks:** Specimens of this species have previously been assigned to the species '*Coccolithites*' *cribellum* Bramlette & Sullivan 1961 and placed in the genera *Cruciplacolithus* and *Clausicoccus* (Prins, 1979; Romein, 1979). The holotype of *cribellum* has narrower shields and a strongly perforate plate and is probably closely allied to, or a junior synonym of, *Clausicoccus fenestratus*. **Differentiation:** Distinguished from other *Clausicoccus* by larger size, relatively wider shield and bright but indistinctly

perforate central area plate. **Dimensions:** Holotype L = 12.7 $\mu$ m (Paratype L = 10.6 $\mu$ m). **Holotype:** Pl. 4, figs 42–43. **Paratype:** Pl. 4, figs 40–41. **Type locality:** IODP Hole U1407A, NW Atlantic Ocean. **Type level:** Middle Eocene, Sample U1407A-10-2, 100cm (Subzone NP14a). **Occurrence:** Subzone NP14a; IODP Site U1407. Difficult to determine its range from published records, which often combine *C. norrisii* and *C. fenestratus*. Reported as NP11–17 by Shamrock & Watkins (2012) for *C. fenestrata*-like specimens >10 $\mu$ m in length.

*Clausicoccus subdistichus* (Roth & Hay in Hay *et al.*, 1967) Prins, 1979

Pl. 4, figs 33–34; Pl. 14, figs 11–12

*Clausicoccus vanheckiae* (Perch-Nielsen, 1986) de Kaenel & Villa, 1996

Pl. 4, figs 38–39

*Hughesius tasmaniae* (Edwards & Perch-Nielsen, 1975) de Kaenel & Villa, 1996

Pl. 4, figs 31–32

Family **CALCIDISCACEAE** Young & Bown, 1997

**Remarks:** We follow the classification of Young & Bown (2014) by placing the majority of Paleogene calcidiscids with closed central-areas in *Calcidiscus* and those with open central-areas in *Umbilicosphaera*. The excellent preservation of the Exp. 342 material reveals the presence of many of the calcidiscid species described from the Tanzania lagerstätte.

*Calcidiscus bicircus* Bown, 2005

Pl. 4, figs 46–47

*Calcidiscus gerrardii* Bown, 2005

Pl. 4, figs 52–53

*Calcidiscus henrikseniae* Bown, 2005

Pl. 4, figs 54–57

*Calcidiscus scullyae* sp. nov.

Pl. 4, figs 48–51

**Derivation of name:** Named after Caitlin Scully (Scripps Institution of Oceanography, USA), Exp. 342 Education Officer. **Diagnosis:** Medium-sized, circular-subcircular placoliths with a non-birefringent distal shield, a narrow, bright tube-cycle and narrow central-area spanned by low-birefringence crossbars. **Differentiation:** Similar to *C. bicircus* but with narrow central area spanned by crossbars (see also Bown, 2005, Pl. 9, figs 21–22). *Calcidiscus parvicrucis* Bown, 2005 is elliptical, has a more distinct tube cycle and a younger range (Lower Eocene). **Dimensions:** Holotype L = 6.3 $\mu$ m (Paratype L = 6.0 $\mu$ m). **Holotype:** Pl. 4, figs 48–49. **Paratype:** Pl. 4, figs 50–51. **Type locality:** IODP Hole U1407A, NW Atlantic Ocean. **Type level:** Middle Eocene, Sample U1407B-8-CC (Subzone NP14b). **Occurrence:** Subzone NP14b; IODP Site U1407 (also Tanzania TDP Site U2; Bown, 2005).

*Umbilicosphaera bramlettei* (Hay & Towe, 1962)

Bown *et al.*, 2007

Pl. 5, figs 7–9; Pl. 14, figs 7–8

**Remarks:** *Umbilicosphaera bramlettei* varies significantly in size through the Eocene and here we distinguish a large variant, with diameter typically greater than 7.5 $\mu$ m. These large coccoliths are very similar to the image named as *Coronocyclus prionion* by Shamrock and Watkins (2012), defined therein as being >7.5 $\mu$ m, but the holotype of *prionion* has a strongly serrated outline and appears to be a *Coronocyclus* coccolith.

*Umbilicosphaera detecta* (de Kaenel & Villa, 1996)

Young & Bown, 2014

Pl. 5, fig. 10

*Umbilicosphaera elliptica* (Shamrock & Watkins, 2012) comb. nov.

Pl. 5, figs 1–3

**Basionym:** *Calcidiscus ellipticus* Shamrock & Watkins, 2012, p. 25, pl. 1, fig. 13. *Stratigraphy*, 9: 1–54. **Remarks:** Following Young and Bown (2014), we place this calcidiscid with open, central area within *Umbilicosphaera*. **Occurrence:** Reported as NP14a-21 in Shamrock and Watkins (2012), we only found unequivocal forms in Subzone NP14b. This morphology is also similar to that seen in *Bramletteius serraculoides* and *Umbilicosphaera detecta*.

*Umbilicosphaera protoannula* (Gartner, 1971) Young &

Bown, 2014

Pl. 5, figs 4–6

#### **Placolith coccoliths *Incertae Sedis***

*Birkelundia arenosa* Perch-Nielsen, 1971

Pl. 5, figs 11–14

*Ellipsolithus lajollaensis* Bukry & Percival, 1971

Pl. 5, figs 16–17

*Markalius latus* Shamrock & Watkins, 2012

Pl. 5, fig. 27

**Remarks:** Large *Markalius* (5.5–9.1 $\mu$ m) with a wide birefringent cycle occupying >33 % of the coccolith diameter (Shamrock and Watkins, 2012). **Occurrence:** NP9/10-14b according to Shamrock and Watkins (2012).

*Pedinocyclus annulus* Shamrock & Watkins, 2012

Pl. 5, figs 20–25

**Remarks:** Medium to large elliptical placolith with a bright inner cycle and open central area. **Occurrence:** Subzone NP14b-21 according to Shamrock & Watkins (2012).

*Tetralithoides symeonidesii* Theodoridis, 1984

Pl. 5, figs 18–19

Coccolith indet. cf. *Hayella* sp.

Pl. 5, figs 27–28

**Description:** High, circular coccolith with relatively bright XPL image and strongly inclined elements. **Occurrence:** Zone NP13, Site U1407.

Coccolith indet. cf. *Scyphosphaera* sp.  
Pl. 5, figs 29–31

**Description:** Very high nannofossil with gently tapering, narrow walls, seen in side view. **Occurrence:** Zone NP13, Site U1407.

Coccolith indet. cf. *Staurolithites* sp.  
Pl. 5, figs 32–33

**Description:** Small coccolith with high, narrow rim and axial cross. **Occurrence:** Zone NP22, Site U1411.

## 10.2 Murolith coccoliths

### 10.2.1 Mesozoic murolith lineages

Order EIFFELLITHALES Rood *et al.*, 1971

Family CHIASTOZYGACEAE Rood *et al.*, 1973

*Jakubowskia leoniae* Varol, 1989

Pl. 5, figs 34–35

*Neocrepidolithus grandiculus* Bown, 2005

Pl. 5, figs 36–37

Family GONIOLITHACEAE Deflandre, 1957

*Goniolithus fluckigeri* Deflandre, 1957

Pl. 5, figs 38–39

### 10.2.2 Cenozoic muroliths

Order ZYGODISCALES Young & Bown, 1997

Family HELICOSPHAERACEAE Black, 1971

*Helicosphaera bramlettei* (Müller, 1970) Jafar & Martini, 1975

Pl. 5, fig. 40; Pl. 14, fig. 16

*Helicosphaera clarissima* Bown, 2005

Pl. 5, fig. 41

*Helicosphaera compacta* Bramlette & Wilcoxon, 1967

Pl. 5, fig. 42; Pl. 14, fig. 19

*Helicosphaera lophota* (Bramlette & Sullivan, 1961)

Locker, 1973

Pl. 5, fig. 43

*Helicosphaera papillata* Bukry & Bramlette, 1969

Pl. 5, fig. 44; Pl. 14, figs 17–18

*Helicosphaera proluxa* sp. nov.

Pl. 5, figs 47–51

**Derivation of name:** From *prolixus*, meaning ‘wide’, referring to the broad overall shape of this species. **Diagnosis:** Large, broadly elliptical *Helicosphaera* with narrow central area spanned by an oblique, disjunct, broad bar. The coccolith is relatively birefringent across the width of the rim. **Differentiation:** Distinguished from other *Helicosphaera* by the broadly elliptical outline and high birefringence image in XPL. **Dimensions:** Holotype L = 10.9 µm (Paratype L = 12.2 µm). **Holotype:** Pl. 5, figs 47–48.

**Paratype:** Pl. 5, figs 49–50. **Type locality:** IODP Hole U1410A, NW Atlantic Ocean. **Type level:** Middle Eocene, Sample U1410A-14H-7, 82cm (Zone NP16). **Occurrence:** Zone NP16; IODP Site U1410.

*Helicosphaera reticulata* Bramlette & Wilcoxon, 1967  
Pl. 5, fig. 45

*Helicosphaera seminulum* Bramlette & Sullivan, 1961  
Pl. 14, fig. 15

*Helicosphaera wilcoxonii* (Gartner, 1971) Jafar & Martini, 1975

Pl. 5, fig. 46; Pl. 14, fig. 14

Family PONTOSPHAERACEAE Lemmermann, 1908

*Pontosphaera alta* Roth, 1970

Pl. 6, fig. 11

*Pontosphaera brinkhuisii* sp. nov.

Pl. 6, fig. 1–4

**Derivation of name:** Named after Dan Brinkhuis (Science Media NL, The Netherlands), Exp. 342 videographer and film maker. **Diagnosis:** Very large, elliptical pontosphaerid with broad, high rim and narrow, apparently vacant central area. **Remarks:** Possibly the taxon that Bralower & Mutterlose (1995) call *Reticulofenestra* “*grandis*” with a reported range of Zones NP15–16. **Differentiation:** Distinguished from other *Pontosphaera* by larger size, thick rim cycles and vacant central area. **Dimensions:** Holotype L = 21.2 µm (Paratype L = 17.1 µm). **Holotype:** Pl. 6, figs 1–2. **Paratype:** Pl. 6, figs 34. **Type locality:** IODP Hole U1409A, NW Atlantic Ocean. **Type level:** Middle Eocene, Sample U1409A-7H-CC (Subzone NP15b). **Occurrence:** Subzone NP15b-16; IODP Sites U1408, U1409

*Pontosphaera clinosulcata* Bown, 2005

Pl. 6, fig. 12

*Pontosphaera enormis* (Locker, 1967) Perch-Nielsen, 1984

Pl. 6, fig. 13

*Pontosphaera exilis* (Bramlette & Sullivan, 1961) Romein, 1979

Pl. 6, fig. 14

*Pontosphaera formosa* (Bukry & Bramlette, 1968) Romein, 1979

Pl. 6, figs 23–24

*Pontosphaera hollisii* sp. nov.

Pl. 6, figs 9–10

**Derivation of name:** Named after Chris Hollis (GNS Science, New Zealand), Exp. 342 shipboard scientist, micropalaeontologist and palaeoceanographer. **Diagnosis:** Very large, broadly elliptical pontosphaerid with broad, low rim and narrow to closed central area. The rim is pale grey in cross-polarised light. **Differentiation:** Distinguished from other *Pontosphaera* by larger size, broad rim cycle and

low birefringence in cross-polarised light. **Dimensions:** Holotype L = 18.1µm (Paratype L = 18.3µm). **Holotype:** Pl. 6, fig. 9. **Paratype:** Pl. 6, fig. 10. **Type locality:** IODP Hole U1409A, NW Atlantic Ocean. **Type level:** Middle Eocene, Sample U1409A-7H-CC (Subzone NP15b). **Occurrence:** Subzone NP15b-c; IODP Site U1409.

*Pontosphaera latoculata* (Bukry & Percival, 1971)  
Perch-Nielsen, 1984  
Pl. 6, figs 15–16

*Pontosphaera multipora* (Kamptner, 1948 ex  
Deflandre, 1954) Roth, 1970  
Pl. 6, fig. 25

*Pontosphaera obliquipons* (Deflandre in Deflandre &  
Fert 1954) Romein 1979  
Pl. 6, fig. 22

*Pontosphaera pulchra* (Deflandre in Deflandre & Fert,  
1954) Romein, 1979  
Pl. 6, fig. 26; Pl. 14, fig. 20

*Pontosphaera romansii* sp. nov.  
Pl. 6, figs 17–21

**Derivation of name:** Named after Brian Romans (Virginia Polytechnic Institute and State University, USA), Exp. 342 shipboard scientist, sedimentologist and palaeoceanographer. **Diagnosis:** Large, narrowly elliptical, lens-shaped pontosphaerid with high rim and apparently vacant central area. **Differentiation:** Distinguished from other pontosphaerids by the high, lens-shaped rim. **Dimensions:** Holotype L = 10.5µm (Paratype L = 11.9µm). **Holotype:** Pl. 6, figs 17–20. **Paratype:** Pl. 6, fig. 21. **Type locality:** IODP Hole U1409A, NW Atlantic Ocean. **Type level:** Middle Eocene, Sample U1409A-8H-CC (Subzone NP15b). **Occurrence:** Subzone NP15b; IODP Site U1409.

*Pontosphaera wilsonii* sp. nov.  
Pl. 6, fig. 5–8

**Derivation of name:** Named after Paul Wilson (University of Southampton, UK), Exp. 342 co-chief scientist and palaeoceanographer. **Diagnosis:** Elliptical pontosphaerid with central area plate crossed by prominent oblique ridges that are bright in cross-polarised light. **Differentiation:** Distinguished from other *Pontosphaera* by the distinctive oblique ridges than run across the coccolith. **Dimensions:** Holotype L = 6.7µm (Paratype L = 7.4µm). **Holotype:** Pl. 6, fig. 6. **Paratype:** Pl. 6, fig. 8. **Type locality:** IODP Hole U1410A, NW Atlantic Ocean. **Type level:** Middle Eocene, Sample U1410A-17X-1, 75cm (Subzone NP15c). **Occurrence:** Subzone NP15b-16; IODP Sites U1408, U1409, U1410.

*Pontosphaera zigzag* (Roth & Hay, 1967 in Hay *et al.*  
1967) comb. nov.  
Pl. 6, figs 27–29

**Basionym:** *Transveropontis zigzag* Roth & Hay, 1967 in Hay *et al.* 1967, p. 450, Plate 7, fig. 4. *Transactions of the Gulf Coast Association of Geological Societies*, 17,

428–480. **Description:** Small *Pontosphaera* with oblique bar usually with a distinct kink and perforate. **Remarks:** Reported as ranging from the middle Eocene (e.g. Self-Trail, 2011) to Oligocene but is often most conspicuous across the Eocene/Oligocene transition. **Occurrence:** Zone NP15c-22; IODP Site U1498, 1410 and 1411. NP14–16 (Self-Trail, 2011).

*Scyphosphaera apsteinii* Lohmann, 1902  
Pl. 6, figs 38–40; Pl. 12, fig. 9; Pl. 14, fig. 21  
*Scyphosphaera columella* Stradner, 1969  
Pl. 6, fig. 36

*Scyphosphaera expansa* Bukry & Percival, 1971  
Pl. 6, fig. 37; Pl. 14, fig. 22

*Scyphosphaera interstincta* sp. nov.  
Pl. 6, figs 30–35

**Derivation of name:** From *interstinctus*, meaning ‘spotted’, referring to the appearance of the wall of this species. **Diagnosis:** Elongate-barrel shaped *Scyphosphaera* with distinct wall ornament of large pits or pores. The coccolith wall tapers gently both proximally and distally, and the inner cycle thickens at the distal opening. **Differentiation:** Distinguished from other *Scyphosphaera* by the wall ornament and inner cycle thickening at the distal opening. **Dimensions:** Holotype L/W = 7.7µm; H = 14.3µm (Paratype L/W = 8.3µm; H = 14.3µm). Holotype L/W = 6.1µm; H = 11.3µm. **Holotype:** Pl. 6, figs 30–31. **Paratype:** Pl. 6, figs 34–35. **Type locality:** IODP Hole U1408A, NW Atlantic Ocean. **Type level:** Upper Eocene, Sample U1408A-14H-5, 63cm (Zone NP16). **Occurrence:** Zone NP15b-16; IODP Sites U1408 and 1409.

Family **ZYGODISCAEAE** Hay & Mohler, 1967  
*Lophodolitus mochlophorus* Deflandre in Deflandre &  
Fert, 1954  
Pl. 8, figs 11–14  
*Lophodolitus rotundus* Bukry & Percival 1971  
Pl. 8, figs 15–16

#### ***Neococcolithes-Nannotetrina* Group** Plate 7; Figure 3

**Description:** Distinctive and unusual coccoliths/nannoliths ranging from simple muroliths (*Isthmolithus*, *Neococcolithes*), through modified-coccoliths with very high and ragged rims (*Chiphragmalithus*), to cruciform and stellate nannoliths, with relict or lost rims (*Nannotetrina*). All share a common crystallographic orientation with crystal units in near-extinction in cross-polarized light, and most are characterised by the presence of diagonally-orientated crossbars. In *Chiphragmalithus* the rim is elevated and often irregular in outline due to lateral outgrowths. In *Nannotetrina* the coccolith rim is lost or relict, and the modified crossbars form the majority of the lith. Throughout the group the coccolith rims or nannoliths are high and often seen in side view (Pl. 7, figs 45–50). **Included**

**genera:** *Chiphragmalithus*, *Isthmolithus*, *Nannotetrina*, *Neococcolithes*. **Occurrence:** Lower Paleocene-Lower Oligocene (Zones NP5?-NP22).

Genus *Chiphragmalithus* Bramlette & Sullivan, 1961  
*Chiphragmalithus acanthodes* Bramlette & Sullivan, 1961

Pl. 7, figs 4–12

**Description:** Elliptical, high rim with lateral projections and central area spanned by diagonal crossbars. The crossbars are high and extend across the rim to the coccolith edge. **Remarks:** Occurs with a number of other unusual coccoliths (e.g. *N. plana*, *N. ruda*) close to the first appearance of the *Nannotetrina* genus (see Section 6). **Occurrence:** Zone NP14a-b; IODP Sites U1408 and U1409.

*Chiphragmalithus calathus* Bramlette & Sullivan, 1961  
 Pl. 7, figs 13–15

**Remarks:** Circular, subcircular or slightly quadrate with simple, high rim and diagonal crossbars. **Occurrence:** Zone NP14; IODP Sites U1408 and U1409.

Genus *Isthmolithus* Deflandre in Deflandre & Fert, 1954

*Isthmolithus recurvus* Deflandre in Deflandre & Fert, 1954

Figure 3

Genus *Nannotetrina* Achuthan & Stradner, 1969  
*Nannotetrina alata* (Martini, 1960) Haq & Lohmann, 1976

Pl. 12, fig. 11

*Nannotetrina cristata* (Martini, 1958) Perch-Nielsen, 1971

Pl. 7, figs 31–43, 50

**Remarks:** We use *N. cristata* here for an array of medium- to large-sized, three-dimensional nannoliths that are broadly cross-shaped with arms that widen towards their ends and with inter-arm fill. They are frequently seen in side view, where they resemble side views of *Chiphragmalithus* (Pl. 7, fig. 50). A small number of specimens observed in Subzone NP14b retain structures that appear to resemble small, square-shaped coccolith rims and central area bars (Pl. 7, figs 37–43).

*Nannotetrina fulgens* (Stradner in Martini & Stradner, 1960) Achuthan & Stradner, 1969

Pl. 12, fig. 12

*Nannotetrina pappii* (Stradner, 1959) Perch-Nielsen, 1971

Figure 3

*Nannotetrina plana* sp. nov.

Pl. 7, figs 21–30

**Derivation of name:** From *planus*, meaning ‘flat’, referring to the relatively flat morphology of this species.

**Diagnosis:** Subcircular to broadly elliptical form comprising a low basal disc crossed by broad, raised crossbars. The constituent elements are in near-extinction in XPL. **Differentiation:** Distinguished from *Nannotetrina cristata* by rounder outline and relatively broader crossbars/ridges that do not thicken and twist at their ends.

**Dimensions:** Holotype L = 9.0 µm (Paratype L = 9.3 µm).

**Holotype:** Pl. 7, figs 21–23. **Paratype:** Pl. 7, figs 25–26.

**Type locality:** IODP Hole U1409A, NW Atlantic Ocean.

**Type level:** Middle Eocene, Sample U1409A-12H-4, 43cm (Subzone NP14b). **Occurrence:** Subzone NP14b; Sites U1408 and U1409.

*Nannotetrina ruda* sp. nov.

Pl. 7, figs 16–20

**Derivation of name:** From *ruda*, meaning ‘rough lump’, referring to the coarse and blocky appearance of this species. **Diagnosis:** Subcircular to broadly elliptical form comprising a rim and high, broad and blocky crossbars. The constituent elements are in near-extinction in XPL.

**Differentiation:** Most similar to *Nannotetrina plana* sp. nov. but blockier in overall form and the crossbars are broader and higher. **Dimensions:** Holotype L = 11.2 µm (Paratype L = 9.8 µm). **Holotype:** Pl. 7, fig. 17. **Paratype:** Pl. 7, fig. 18. **Type locality:** IODP Hole U1409A, NW Atlantic Ocean. **Type level:** Middle Eocene, Sample U1409A-12H-4, 43cm (Subzone NP14b). **Occurrence:** Zone NP14b; IODP Site U1409.

*Nannotetrina spinosa* (Stradner in Martini & Stradner, 1960) Bukry, 1973

Pl. 7, fig. 44

Genus *Neococcolithes* Sujkowski, 1931

*Neococcolithes dubius* (Deflandre in Deflandre & Fert, 1954) Black, 1967

Pl. 7, fig. 1; Pl. 14, fig. 23

*Neococcolithes protenus* (Bramlette & Sullivan, 1961) Black, 1967

Pl. 7, figs 2–3, 45

**Remarks:** Elliptical, simple rim with diagonal crossbars.

*Neococcolithes purus* sp. nov.

Pl. 8, figs 8–10

**Derivation of name:** From *purus*, meaning ‘plain’, referring to the apparently vacant central area of this species.

**Diagnosis:** Narrowly-elliptical murolith coccolith with a narrow, low birefringence, unicyclic rim image and relatively wide, apparently vacant, central area. **Remarks:** To date, its distribution is the same as that of *Neococcolithes radiatus* sp. nov. **Differentiation:** Distinguished from other species of *Neococcolithes* by the vacant central area. Similar in overall form to *Jakubowskia leoniae* Varol,

1989 but it is smaller, has a narrower, low birefringence rim and a different stratigraphic range. **Dimensions:** Holotype L = 6.8  $\mu\text{m}$  (Paratype L = 5.7  $\mu\text{m}$ ). **Holotype:** Pl. 8, figs 8–9. **Paratype:** Pl. 8, fig. 10. **Type locality:** IODP Hole U1410A, NW Atlantic Ocean. **Type level:** Middle Eocene, Sample U1410A-7H-CC (Zone NP17). **Occurrence:** Zone NP17; IODP Sites U1408, U1410.

*Neococcolithes radiatus* sp. nov.

Pl. 8, figs 1–7

**Derivation of name:** From *radiatus*, meaning ‘with rays’, referring to the grill in the central area of this species. **Diagnosis:** Narrowly-elliptical murolith coccolith with a low birefringence, unicyclic rim image and central area with numerous (around 18–22) radiating bars. **Description:** The rim shows relatively low birefringence in XPL as do the central area bars. Some specimens have outlines approaching rhomboidal. **Remarks:** The rhomboidal outline and stratigraphic position close to the extinction of *Neococcolithes dubius* and first appearance of *Isthmolithus recurvus* suggest that this may be a transitional species between the two genera. **Differentiation:** Distinguished from most other species of *Neococcolithes*, which have diagonal crossbars, by the more numerous central area bars. **Dimensions:** Holotype L = 7.6  $\mu\text{m}$  (Paratype L = 6.4  $\mu\text{m}$ ). **Holotype:** Pl. 8, figs 1–4. **Paratype:** Pl. 8, figs 5–7. **Type locality:** IODP Hole U1410A, NW Atlantic Ocean. **Type level:** Middle Eocene, Sample U1410A-7H-CC (Zone NP17). **Occurrence:** Zone NP17; IODP Site U1410.

Family **RHABDOSPHAERACEAE** Haeckel, 1894

Genus *Blackites* Hay & Towe, 1962

*Blackites* bases

Pl. 8, figs 17–39

**Remarks:** In well preserved material *Blackites* bases can be common components of nannofossil assemblages, albeit inconspicuous because of their low birefringence images in XPL. They represent both the disarticulated bases of spinose forms, together with non-spinose coccoliths, such as *B. amplus* and *B. furvus*. Small *Blackites* bases (Pl. 8, figs 22–23) are common through the middle to late Eocene of the Exp. 342 sites and are most likely the disarticulated bases of the common species *B. spinosus* and *B. tenuis*.

*Blackites amplus* Roth & Hay, 1967

Pl. 8, figs 17–21

*Blackites creber* (Deflandre in Deflandre & Fert, 1954)

Sherwood, 1974

Pl. 9, fig. 9

*Blackites deflandrei* (Perch-Nielsen 1968) Bown, 2005

var. 1

Pl. 8, figs 42, 43, 47; Pl. 15, figs 1–2

**Remarks:** *Blackites* with broad coccolith base and broad, thin-walled, variably tall, dome-like to bullet-shaped

spine. The spine is ornamented and parallel-sided in its lower part before tapering to a point. In SEM the ornamentation is revealed to be perforations/windows. The species was originally defined and illustrated as having variable spine height but the complete type specimens have a height less than the coccolith rim width. Here we distinguish two informal varieties based on spine height: variety 1 with height < coccolith rim width and variety 2 with height > coccolith rim width.

*Blackites deflandrei* (Perch-Nielsen 1968) Bown, 2005

var. 2

Pl. 8, figs 48–52

**Remarks:** Like *B. deflandrei* var. 1 but with spine height > coccolith rim width. **Occurrence:** Zone NP16–19/20; IODP Site U1410, U1411.

*Blackites dupuisii* (Steurbaut, 1990) Bown, 2005

Pl. 8, figs 53–55

*Blackites friedrichii* sp. nov.

Pl. 8, figs 29–39

**Derivation of name:** Named after Oliver Friedrich (University of Heidelberg, Germany), Exp. 342 shipboard scientist, micropalaeontologist and palaeoceanographer. **Diagnosis:** *Blackites* with broad circular base and broad, low, thin-walled, globular spine with distinct image in XPL having a crenulate edge and strong extinction cross. Typically seen in plan view. **Differentiation:** Distinguished from most *Blackites* bases by its large diameter and from *B. amplus* by its distinctive, low, globular spine. **Dimensions:** Holotype L = 5.4  $\mu\text{m}$  (Paratype L = 4.5  $\mu\text{m}$ ). **Holotype:** Pl. 7, fig. 33. **Paratype:** Pl. 7, fig. 30. **Type locality:** IODP Hole U1408C, NW Atlantic Ocean. **Type level:** Middle Eocene, Sample U1408C-10X-3, 63cm (Zone NP16). **Occurrence:** Zones NP16–17; IODP Site U1408, U1409, U1410.

*Blackites furvus* Bown & Dunkley Jones, 2006

Pl. 8, figs 24–28

*Blackites gladius* (Locker, 1967) Varol, 1989

Pl. 9, figs 5–6; Pl. 15, fig. 3

*Blackites globosus* Bown, 2005

Pl. 8, figs 56–58

*Blackites* cf. *B. herculesii* (Stradner, 1969) Bybell &

Self-Trail, 1997

Pl. 9, figs 35–39

**Remarks:** Tall, narrow, club-like, disarticulated *Blackites* spines that narrow towards both ends and which have a dark image in XPL. **Occurrence:** Zones 15b–17; Site U1409.

*Blackites inflatus* (Bramlette & Sullivan, 1961)

Kapellos & Schaub, 1973

Pl. 9, figs 10, 30

*Blackites inversus* (Bukry & Bramlette, 1969) comb. nov.  
Pl. 9, fig. 26

**Basionym:** *Triquetrorhabdulus inversus* Bukry & Bramlette, 1969, Some new and stratigraphically useful calcareous nannofossils of the Cenozoic. *Tulane Studies in Geology*, 7: p.142, pl. 1, figs 9–14. **Description:** Very long spinose forms that taper towards each end and which have undulating outline and narrow axial canal. In XPL they are dark at 0° and bright at 45°. **Remarks:** Previously placed in *Triquetrorhabdulus* by Bukry & Bramlette (1969) and *Pseudotriquetrorhabdulus* by Wise (in Wise & Constans, 1976), these spinose forms occur alongside other *Blackites* spines with similar LM image and crystallographic orientation, and they most likely represents a *Blackites* species that readily detaches from its coccolith base. It can occur abundantly and has a relatively restricted stratigraphic range in the middle Eocene (Zones NP14–15), with a particular acme interval in Zone NP14 (Backman, 1986). **Occurrence:** Zones NP14–15.

*Blackites kilwaensis* Bown, 2005  
Pl. 9, fig. 12

*Blackites ornatus* Bown & Dunkley Jones, 2006  
Pl. 9, fig. 13

*Blackites perlongus* (Deflandre, 1952) Shafik, 1981  
Pl. 9, figs 22–23

*Blackites piriformis* (Pavsic in Khan *et al.*, 1975)  
Aubry, 1999  
Pl. 9, fig. 11

*Blackites pseudomorionum* (Locker 1967) Aubry 1999  
Pl. 8, fig. 46

*Blackites* cf. *B. pseudomorionum* (Locker 1967) Aubry 1999  
Pl. 8, figs 44–45  
*Blackites rotundus* Bown, 2005  
Pl. 9, figs 7–8

*Blackites sextonii* sp. nov.  
Pl. 9, figs 1–4

**Derivation of name:** Named after Phil Sexton (Open University, UK), Exp. 342 shipboard scientist, micropalaeontologist and palaeoceanographer. **Diagnosis:** *Blackites* with broad base, and very tall, broad, thin-walled spine. The broad spine is near-parallel sided or very gently tapering for most of its length before tapering sharply to a point. **Differentiation:** Distinguished from other *Blackites* by its broad, very tall spine. **Dimensions:** Holotype max coccolith base W = 5.9µm; spine L = 13.1µm, spine W = 2.3µm (Paratype spine L = 12.7µm). **Holotype:** Pl. 8, fig. 1. **Paratype:** Pl. 8, figs 3, 4. **Type locality:** IODP Hole U1408C, NW Atlantic Ocean. **Type level:** Upper Eocene, Sample U1408C-7H-4, 93cm (Zone NP16). **Occurrence:** Zone NP16; IODP Site U1408.

*Blackites subtilis* sp. nov.  
Pl. 9, figs 27–29

**Derivation of name:** From *subtilis*, meaning ‘slender’, referring to the very narrow form of this spine. **Diagnosis:** Very long, slender spine that is near-parallel-sided with a narrow axial canal. In XPL, the spine is dark when parallel with the polarising directions and bright at 45°. It is typically seen with no basal coccolith. **Differentiation:** Most likely a spine of the genus *Blackites*, but distinguished from other narrow-spined species, such as *B. perlongus* and *B. tenuis*, by its length, very narrow axial canal and lack of taper. **Dimensions:** Holotype spine L = 22.4µm, spine W = 1.2µm (Paratype minimum L = 16.1µm, spine W = 1.2µm). **Holotype:** Pl. 9, fig. 27. **Paratype:** Pl. 9, fig. 28. **Type locality:** IODP Hole U1407A, NW Atlantic Ocean. **Type level:** Upper Eocene, Sample U1407A-9H-6, 57cm (Subzone NP14b). **Occurrence:** Subzone NP14b–Zone NP16; IODP Sites U1407, U1408 and U1409.

*Blackites spinosus* (Deflandre & Fert, 1954) Hay & Towe, 1962

Pl. 9, figs 31–32; Pl. 15, fig. 4

*Blackites* cf. *B. spinosus* (Deflandre & Fert, 1954) Hay & Towe, 1962  
Pl. 9, fig. 21

*Blackites stilus* Bown, 2005  
Pl. 9, figs 24–25

*Blackites tenuis* (Bramlette & Sullivan 1961)  
Sherwood, 1974  
Pl. 9, figs 33–34; Pl. 15, fig. 5

*Blackites tortilis* Bown & Dunkley Jones, 2006  
Pl. 9, figs 16–20; Pl. 15, fig. 6

*Blackites virgatus* Bown, 2005  
Pl. 9, figs 14–15

*Rhabdosphaera gracilentia* (Bown & Dunkley Jones, 2006) Dunkley Jones *et al.*, 2009  
Pl. 9, figs 40–44

**Remarks:** Transferred from *Blackites* to *Rhabdosphaera* by Dunkley Jones *et al.* (2009) but spelt *gracilentus*. Orthography corrected here.

*Rhabdosphaera vitrea* (Deflandre in Deflandre & Fert 1954) Bramlette & Sullivan, 1961  
Pl. 9, figs 45–48

#### Order SYRACOSPHAERALES Hay, 1977 emend. Young *et al.*, 2003

Family CALCIOSOLENIACEAE Kamptner, 1927  
*Calciosolenia alternans* Bown & Dunkley Jones, 2006  
Pl. 9, fig. 49

Family SYRACOSPHAERACEAE Lemmermann, 1908

*Syracosphaera octiforma* sp. nov.  
Pl. 9, figs 51–54

**Derivation of name:** From *octi*, meaning ‘eight’, and ‘*forma*’ meaning form, referring to the distinctive outline

of this species. **Diagnosis:** Narrow rimmed coccolith with figure-of-eight outline (indentations on each side). In XPL the rim is relatively bright and there may be a spine in the central area, which is otherwise unclear. **Remarks:** We tentatively assign this species to *Syracosphaera* based on the rim image in XPL. **Differentiation:** Distinguished from most other coccoliths by its distinctive outline. **Dimensions:** Holotype L = 5.5  $\mu\text{m}$  (Paratype L = 5.2  $\mu\text{m}$ ). **Holotype:** Pl. 9, figs 53–54. **Paratype:** Pl. 9, figs 51–52. **Type locality:** IODP Hole U1408A, NW Atlantic Ocean. **Type level:** Upper Eocene, Sample U1408A-4H-CC (Zone NP17). **Occurrence:** Zone NP16–17; IODP Sites U1408, U1410.

*Syracosphaera tanzanensis* Bown, 2005

Pl. 8, fig. 50

#### **Murolith coccoliths *Incertainae* Sedis**

*Pocillithus spinulifer* Dunkley Jones *et al.*, 2009

Pl. 15, figs 7–8

### **10.3 Holococcoliths**

Family CALYPTROSPHAERACEAE Boudreaux & Hay, 1967

*Daktylethra punctulata* Gartner in Gartner & Bukry, 1969

Pl. 10, figs 4–6

*Daktylethra unitatis* Bown & Dunkley Jones, 2006

Pl. 10, figs 1–3; Pl. 15, fig. 9

*Holodiscolithus agniniae* sp. nov.

Pl. 10, figs 14–21

**Derivation of name:** Named after Claudia Agnini (University of Padua, Italy), Exp. 342 shipboard scientist, nanopalaeontologist and biostratigrapher. **Remarks:** Flat, elliptical holococcolith formed from six crystallographic blocks divided by near-radial sutures. **Differentiation:** Similar to Cretaceous coccoliths of the genus *Calculites*, but this species is distinguished by being flat and having six similarly-sized crystallographic blocks. **Dimensions:** Holotype L = 4.9  $\mu\text{m}$  (Paratype L = 4.8  $\mu\text{m}$ ). **Holotype:** Pl. 9, figs 17–19. **Paratype:** Pl. 9, figs 14–16. **Type locality:** IODP Hole U1407A, NW Atlantic Ocean. **Type level:** Middle Eocene, Sample U1407A-9H-6, 58cm (Subzone NP14b). **Occurrence:** Subzone NP14b; IODP Site U1407.

*Holodiscolithus lippertii* sp. nov.

Pl. 10, figs 33–38

**Derivation of name:** Named after Peter Lippert (University of Utah, USA), Exp. 342 shipboard scientist, palaeomagnetist and palaeoceanographer. **Diagnosis:** Small, elliptical, moderately-birefringent holococcolith crossed by roughly diagonal extinction lines in XPL delineating four blocks, which are birefringent at 0° and dark at 45°. There are around 8–10 perforations across the blocks and raised axial ridges are visible in phase contrast.

**Differentiation:** The perforations are smaller than *Holodiscolithus solidus* and less numerous than *Holodiscolithus macroporus*. **Dimensions:** Holotype L = 3.2  $\mu\text{m}$  (Paratype L = 3.4  $\mu\text{m}$ ). **Holotype:** Pl. 10, figs 36–38. **Paratype:** Pl. 10, figs 33–35. **Type locality:** IODP Hole U1411B, NW Atlantic Ocean. **Type level:** Eocene/Oligocene transition, Sample U1411C-8H-6, 60cm (Zone NP21). **Occurrence:** Zone NP21; IODP Site U1411.

*Holodiscolithus liui* sp. nov.

Pl. 10, figs 22–26

**Derivation of name:** Named after Zhonghui Liu (Department of Earth Sciences, University of Hong Kong), Exp. 342 shipboard scientist, geochemist and palaeoceanographer. **Diagnosis:** Small, elliptical holococcolith with narrow rim and broad bar that almost fills the central area; the bar is dark at 0° and birefringent at 45°. **Differentiation:** Similar to *H. serus* but is more regular in outline and shows no perforations. **Dimensions:** Holotype L = 3.9  $\mu\text{m}$  (Paratype L = 3.9  $\mu\text{m}$ ). **Holotype:** Pl. 10, figs 24–26. **Paratype:** Pl. 10, fig. 22. **Type locality:** IODP Hole U1407A, NW Atlantic Ocean. **Type level:** Middle Eocene, Sample U1407A-9H-6, 57cm (Subzone NP14b). **Occurrence:** Subzone NP14b; IODP Site U1407.

*Holodiscolithus solidus* (Deflandre in Deflandre &

Fert, 1954) Roth, 1970

Pl. 10, figs 9–13; Pl. 15, fig. 10

*Holodiscolithus whitesideae* sp. nov.

Pl. 10, figs 27–30

**Derivation of name:** Named after Jessica Whiteside (University of Southampton, UK), Exp. 342 shipboard scientist, geochemist and palaeoceanographer. **Diagnosis:** Small holococcolith seen in side view, with steep-sided base and short, narrow spine. All parts of the holococcolith show similar crystallographic orientation and it is moderately birefringent at 45°, and dark at 0°. A median septum appears to be present. **Differentiation:** **Dimensions:** Holotype L = 3.1  $\mu\text{m}$ , H = 3.3  $\mu\text{m}$  (Paratype L = 2.8  $\mu\text{m}$ , H = 2.9  $\mu\text{m}$ ). **Holotype:** Pl. 10, figs 27–28. **Paratype:** Pl. 10, figs 29–30. **Type locality:** IODP Hole U1408C, NW Atlantic Ocean. **Type level:** Middle Eocene, Sample U1408C-10H-3, 63cm (Zone NP16). **Occurrence:** Zone NP16; IODP Site U1408.

*Lanternithus minutus* Stradner, 1962

Pl. 10, figs 7–8; Pl. 15, fig. 11

*Semihololithus pseudobiskayae* sp. nov.

Pl. 10, figs 39–44

**Derivation of name:** From the Greek word *pseudes*, meaning ‘false’, and referring to its similarity to the older, Paleocene species *Semihololithus biskayae*. **Diagnosis:** Large, blocky coccolith seen in side view, with steep-walled rim and domed upper surface. **Differentiation:**

Similar in overall shape to *Semihololithus biskayae* but has a more irregular appearance, lower birefringence image and blockier upper cover. **Dimensions:** Holotype L = 6.6µm, H = 6.5µm (Paratype L = 6.6µm, H = 6.8µm). **Holotype:** Pl. 10, fig. 43–44. **Paratype:** Pl. 10, figs 41–42. **Type locality:** IODP Hole U1407A, NW Atlantic Ocean. **Type level:** Middle Eocene, Sample U1407A-9H-6, 57cm (Subzone NP14b). **Occurrence:** Subzone NP14b; IODP Sites U1407 and U1408.

*Zygrhablithus bijugatus bijugatus* (Deflandre in Deflandre & Fert, 1954) Deflandre, 1959  
Pl. 10, figs 45–50; Pl. 15, fig. 12

Holococcolith sp. indet.  
Pl. 10, figs 31–32

**Remarks:** Small, elliptical holococcolith with transverse bar, displaying a low birefringence image in XPL and high relief in PC. Occurrence: Middle Eocene, Subzone NP14b; Site U1407.

## 10.4 Extinct nannoliths

### Order DISCOASTERALES Hay, 1977 emend. Bown, 2010

#### Family DISCOASTERACEAE Tan, 1927

*Discoaster barbadiensis* Tan, 1927

Pl. 15, fig. 14

*Discoaster distinctus* Martini, 1958

Pl. 15, fig. 17

*Discoaster martinii* Stradner, 1959

Pl. 12, fig. 10

*Discoaster nodifer* (Bramlette & Riedel, 1954) Bukry, 1973

Pl. 15, figs 15, 18

*Discoaster saipanensis* Bramlette & Riedel, 1954

Pl. 15, fig. 13

#### Family SPHENOLITHACEAE Deflandre, 1952

##### *Sphenolithus furcatolithoides* Subgroup

Pl. 11, figs 1–29

**Remarks:** Included within the *S. radians* group by Bown & Dunkley Jones (2012), these species are characterised by two (rarely more) bifurcating apical spines, bright at 0° and dark at 45°, extending from the upper quadrants. Species differentiation is based on the height and angle of spine bifurcation and size of the basal quadrants. In moderate to poor preservation the upper portion of these tall spines is usually lost, but when well preserved, as seen herein, the entire lith may be preserved, highlighting the extreme spine lengths (up to 25µm; Pl. 11, fig. 25) and variations in upper spine morphology. Morphology within the group includes:

1. *S. kempii* – square base with three of four spines;
2. *S. cf. S. perpendicularis* – tapering base with narrow, high-angled lateral spines;
3. *S. perpendicularis* Shamrock, 2010 – square base with two spines that diverge by around 90°;

4. *S. furcatolithoides* – spines diverge just above the base and are near-parallel in the lower part;
5. *S. cuniculus* – forms with low basal quadrants (‘feet’) and ~90° bifurcations; and
6. *S. strigosus* – duocrystalline spines that bifurcate high-up on the spine.

In the slightly younger, and probably descendant, *S. predistentus* group, only the lower quadrants are clearly discernable in the basal column and the spines are bright at 45° and diverge in the uppermost part of the spine (e.g. *S. obtusus*, *S. runus*, *S. predistentus*).

*Sphenolithus cuniculus* Bown, 2005  
Pl. 11, figs 19–20, 25

*Sphenolithus furcatolithoides* Locker 1967

Pl. 11, figs 15–18, 21–22, 26

**Description:** Typified by two apical spines that extend and diverge from the upper basal quadrants but that are near-parallel in the lower, normally preserved, part. When preservation is very good, the upper part of the spines are preserved and may be near-parallel or diverge from the long axis of the sphenolith by varying amounts. Variants include small, gracile forms with near-parallel bifurcations that bend to form higher degree (>90°) bifurcations high on the spine (Pl. 11, fig. 26), and forms with upper spines that converge (Pl. 11, fig. 22). Specimens at the base of the species range at Site U1410 appear most similar to *S. radians* (Pl. 11, figs 14–15).

*Sphenolithus cf. S. kempii* sensu Bown & Dunkley Jones, 2012  
Pl. 11, figs 4–6

*Sphenolithus perpendicularis* Shamrock, 2010

Pl. 11, figs 9–13

**Description:** Sphenolith with two apical spines that diverge by ~90° (45° to the sphenolith long axis) just above the basal cycles. Restricted to Subzone NP15a according to Shamrock (2010). Informally identified as *Sphenolithus “spinatus”* by Bralower & Mutterlose (1995) and shown ranging from upper Subzone NP14b to Subzone NP15b. The *S. perpendicularis*-like forms seen in the Exp. 342 material have narrower spines but this may be due to overgrowth in the type material. Forms where the spines make a distinct angle with the upper basal quadrant are distinguished as *Sphenolithus cf. S. perpendicularis* herein. **Occurrence:** Subzone NP14b–15b. Sites U1407, U1408.

*Sphenolithus cf. S. perpendicularis* Shamrock, 2010  
Pl. 11, figs 1–3

**Description:** Short, squat sphenoliths with a base formed from broad, gently-tapering lower quadrants and smaller upper quadrants. Two long, narrow, lateral spines emerge

from the upper quadrants making an angle of around 160° (80° to the sphenolith long axis). **Differentiation:** The base is most similar to *S. moriformis* or *S. spiniger* but this species is distinguished from these by long lateral spines. The spines are most similar to *S. furcatolithoides* group sphenoliths, but are narrower and emerge from the base at a higher angle. **Occurrence:** Subzone NP14b-15b. Site U1408.

*Sphenolithus strigosus* Bown & Dunkley Jones 2006  
Pl. 11, figs 23, 27–29; Pl. 15, fig. 22

#### ***Sphenolithus predistentus* Group**

Pl. 11, figs 30–43

**Remarks:** These species are characterised by a base with two, low quadrants (or ‘feet’) and tapering duo- or monocrystalline spines with terminal bifurcations that may be very long. The spines are visible but dim at 0° and brightest when at 45° to the polarizing directions.

*Sphenolithus obtusus* Bukry 1971  
Pl. 11, figs 36–38, 40–41; Pl. 15, fig. 21  
*Sphenolithus predistentus* Bramlette & Wilcoxon 1967  
Pl. 11, figs 42–43

*Sphenolithus runus* Bown & Dunkley Jones 2006  
Pl. 11, figs 30–35

**Remarks:** Similar to *S. obtusus* but the spine is dark at 0° and does not appear duocrystalline at 45°.

#### **Other sphenoliths**

*Sphenolithus moriformis* (Brönnimann & Stradner, 1960) Bramlette & Wilcoxon, 1967  
Pl. 15, fig. 19

*Sphenolithus radians* Deflandre in Grassé 1952  
Pl. 15, fig. 16

*Sphenolithus spiniger* Bukry 1971  
Pl. 15, fig. 20

*Sphenolithus* spines  
Pl. 11, figs 24, 39, 44–45

**Remarks:** Several middle Eocene sphenoliths have very tall spines which, when well preserved, retain even longer, usually bifurcating, terminal spine ends (e.g. *S. cuniculus*, *S. furcatolithoides*, *S. obtusus*, *S. strigosus*). These spines may reach up to 32 µm in length, and in *S. furcatolithoides* they take on a variety of different shapes, with up to two inflection points. In a number of stratigraphic intervals narrow spine-like liths are common and may represent broken sphenolith spines. However, in some case these liths have triradiate form, which do not appear to have been sourced from sphenoliths (Pl. 11, figs 39, 45).

#### **Incertae Sedis Nannoliths**

*Leesella procera* Bown & Dunkley Jones, 2006  
Pl. 11, figs 46–48

## **Acknowledgements**

Thanks to IODP Expedition 342 operational and technical staff and shipboard science party for facilitating such an enjoyable and successful drilling expedition. This research used samples provided by the Integrated Ocean Drilling Program (IODP). Funding for this research was provided to PB (Expedition participation) and CN (PhD studentship) by the Natural Environment Research Council (NERC).

## **References**

- Agnini, C., Muttoni, G., Kent, D.V. & Rio, D. 2006. Eocene biostratigraphy and magnetic stratigraphy from Possagno, Italy: The calcareous nannofossil response to climate variability. *Earth and Planetary Science Letters*, **241**: 815–830.
- Agnini, C., Fornaciari, E., Raffi, I., Catanzariti, R., Pälike, H., Backman, J., Rio, D. 2014. Biozonation and biochronology of Paleogene calcareous nannofossils from low and middle latitudes. *Newsletters on Stratigraphy*, **47**: 131–181.
- Backman, J. 1986. Late Paleocene to middle Eocene calcareous-nannofossil biochronology from the Shatsky Rise, Walvis Ridge and Italy. *Palaeogeography, Palaeoclimatology, Palaeoecology*, **57**: 43–59.
- Backman, J. & Hermelin, J.O.R. 1986. Morphometry of the Eocene nannofossil *Reticulofenestra umbilicus* lineage and its biochronological consequences. *Palaeogeography, Palaeoclimatology, Palaeoecology*, **57**: 103–116.
- Bown, P.R. (Ed.) 1998. *Calcareous Nannofossil Biostratigraphy*. Kluwer Academic, London: 315pp.
- Bown, P.R., 2005. Palaeogene calcareous nannofossils from the Kilwa and Lindi areas of coastal Tanzania (Tanzania Drilling Project 2003–4). *Journal of Nannoplankton Research*, **27**: 21–95.
- Bown, P.R. 2010. Calcareous nannofossils from the Paleocene/Eocene Thermal Maximum interval of southern Tanzania (TDP Site U14). *Journal of Nannoplankton Research*, **31**: 11–38.
- Bown, P.R. 2016. Paleocene calcareous nannofossils from Tanzania (TDP sites U19, U27 and U38). *Journal of Nannoplankton Research*, **36**: 1–32.
- Bown, P.R. & Young, J.R. 1998. Techniques. In: P.R. Bown (Ed.). *Calcareous Nannofossil Biostratigraphy*. Kluwer Academic, London: 16–28.
- Bown, P.R. & Dunkley Jones, T. 2006. New Paleogene calcareous nannofossil taxa from coastal Tanzania: Tanzania Drilling Project Sites U11 to U14. *Journal of Nannoplankton Research*, **28**: 17–34.
- Bown, P.R. & Dunkley Jones, T. 2012. Calcareous nannofossils from the Paleogene equatorial Pacific (IODP Expedition 320 Sites U1331–1334). 2012. *Journal of Nannoplankton Research*, **32**: 3–51.
- Bown, P.R., Dunkley Jones, T., Young, J.R. 2007. *Umbilicosphaera jordanii* Bown, 2005 from the Paleogene of Tanzania: confirmation of generic assignment and a Paleocene origination for the family Calcidiscaceae. *Journal of Nannoplankton Research*, **29**: 25–30.

- Bown, P.R., Dunkley-Jones, T., Lees, J.A., Randell, R.D., Mizzi, J.A., Pearson, P.N., Coxall, H.K., Young, J.R. *et al.* 2008. A Paleogene Calcareous microfossil Konservat-Lagerstätte from the Kilwa Group of coastal Tanzania. *GSA Bulletin*, **120**: 3–12.
- Bralower, T.J. & Mutterlose, J. 1995. Calcareous nannofossil biostratigraphy of Site U865, Allison Guyot, Central Pacific Ocean: a tropical Paleogene reference section. *Proceedings of the ODP, Scientific Results*, **143**: 31–74.
- Bramlette, M.N. & Sullivan, F.R. 1961. Coccolithophorids and related Nannoplankton of the early Tertiary in California. *Micropaleontology*, **7**: 129–188.
- Bukry, D. & Bramlette, M.N. 1969. Some new and stratigraphically useful calcareous nannofossils of the Cenozoic. *Tulane Studies in Geology and Paleontology*, **7**: 131–142.
- Dunkley Jones, T., Bown, P.R. & Pearson, P.N. 2009. Exceptionally well preserved upper Eocene to lower Oligocene calcareous nannofossils from the Pande Formation (Kilwa Group), Tanzania. *Journal of Systematic Palaeontology*, **7**: 359–411.
- Fornaciari, E., Agnini, C., Catanzariti, R., Rio, D., Bolla, E.M. & Valvasoni, E. 2010. Mid-Latitude calcareous nannofossil biostratigraphy and biochronology across the middle to late Eocene transition. *Stratigraphy*, **7**: 229–264.
- Gibbs, S.J., Bralower, T.J., Bown, P.R., Zachos, J. & Bybell, L.M., 2006. Decoupled shelf-ocean phytoplankton productivity responses across the Paleocene-Eocene Thermal Maximum. *Geology*, **34**: 233–236.
- Gibbs, S.J., Bown, P.R., Ridgwell, A., Young, J.R., Poulton, A.J. & O'Dea, S.A. 2016. Ocean warming not acidification controls coccolithophore response during past greenhouse climate change. *Geology*, **44**: 59–62.
- Gradstein, F.M., Ogg, J.G., Schmitz, M., Ogg, G. (Eds) 2012. *The Geological Time Scale 2012*. Elsevier. ISBN: 978-0-444-59425-9.
- Jordan, R.W., Kleijne, A. & Young, J.R. 2004. A revised classification scheme for living haptophytes. *Micropaleontology*, **50**: 55–79.
- Kelly, D.C., Norris, R.D. & Zachos, J.C. 2003. Deciphering the paleoceanographic significance of Early Oligocene *Braarudosphaera* chalks in the South Atlantic. *Marine Micropaleontology*, **49**: 49–63.
- Martini, E. 1971. Standard Tertiary and Quaternary calcareous nannoplankton zonation. In: A. Faranacci (Ed.). *Proceedings of the Second Planktonic Conference Roma 1970*. Edizioni Tecnoscienza, Rome, **2**: 739–785.
- Nannotax3 - Young, J.R., Bown P.R. & Lees J.A. (Eds). *Nannotax3 website*. International Nannoplankton Association. May 2014. URL: <http://www.mikrotax.org/Nannotax3/>.
- Norris, R.D., Wilson, P.A., Blum, P. & the Expedition 342 Scientists, 2014. Paleogene Newfoundland Sediment Drifts and MDHDS Test. *Proceedings of the IODP*, **342**: College Station, TX (Integrated Ocean Drilling Program). doi: 10.2204/iodp.proc.342.2014 [<http://publications.iodp.org/proceedings/342/342title.htm>].
- Perch-Nielsen, K., 1985. Cenozoic calcareous nannofossils. In: H.M. Bolli, J.B. Saunders & K. Perch-Nielsen (Eds). *Plankton Stratigraphy*. Cambridge University Press, Cambridge: 427–554.
- Prins, B., 1979. Notes on nannology 1. *Clausiococcus*, a new genus of fossil Coccolithophorids. *INA Newsletter*, **1**: N2–N4.
- Romein, A.J.T. 1979. Lineages in early Paleogene calcareous nannoplankton. *Utrecht Micropaleontological Bulletins*, **22**: 1–230.
- Schneider, L.J., Bralower, T.J. & Kump, L.R., 2011. Response of nannoplankton to early Eocene ocean destratification. *Palaeogeography, Palaeoclimatology, Palaeoecology*, **310**: 152–162.
- Shamrock, J.L. 2010. A new calcareous nannofossil species of the genus *Sphenolithus* from the Middle Eocene (Lutetian) and its biostratigraphic significance. *Journal of Nannoplankton Research*, **31**: 5–10.
- Shamrock, J.L. & Watkins, D.K. 2012. Eocene calcareous nannofossil biostratigraphy and community structure from Exmouth Plateau, Eastern Indian Ocean (ODP Site U762). *Stratigraphy*, **9**: 1–54.
- Wei, W. 1993. Clarification of *Coccolithus crassus* Bramlette & Sullivan, an index fossil of coccolithophorida. *Journal of Paleontology*, **67**: 135–138.
- Wise, S.W. & Constans, R.E. 1976. Mid Eocene plankton correlations Northern Italy - Jamaica W.I. *Transactions of the Gulf Coast Association of Geological Societies*, **26**: 144–155.
- Young, J.R. 1990. Size variation of Neogene *Reticulofenestra* coccoliths from the Indian Ocean DSDP cores. *Journal of Micropalaeontology*, **9**: 71–85.
- Young, J.R. 1998. Neogene. In: P.R. Bown (Ed.). *Calcareous Nannofossil Biostratigraphy*. Kluwer Academic, London: 225–265.
- Young, J.R. & Bown, P.R. 1997. Cenozoic calcareous nannoplankton classification. *Journal of Nannoplankton Research*, **19**: 36–47.
- Young, J.R. & Bown, P.R. 2014. Some emendments to calcareous nannoplankton taxonomy. *Journal of Nannoplankton Research*, **33**: 39–46.
- Young, J.R., Bergen, J.A., Bown, P.R., Burnett, J.A., Fiorentino, A., Jordan, R.W., Kleijne, A., van Niel, B.E. *et al.* 1997. Guidelines for coccolith and calcareous nannofossil terminology. *Palaeontology*, **40**: 875–912.
- Young, J.R., Geisen, M., Cros, L., Kleijne, A., Sprengel, C., Probert, I. & Ostergaard, J. 2003. A guide to extant coccolithophore taxonomy. *Journal of Nannoplankton Research Special Issue 1*: 125pp.
- Young, J.R., Geisen, M., & Probert, I. 2005. A review of selected aspects of coccolithophore biology with implications for palaeodiversity estimates. *Micropaleontology*, **51**: 267–288.

## Plate 1

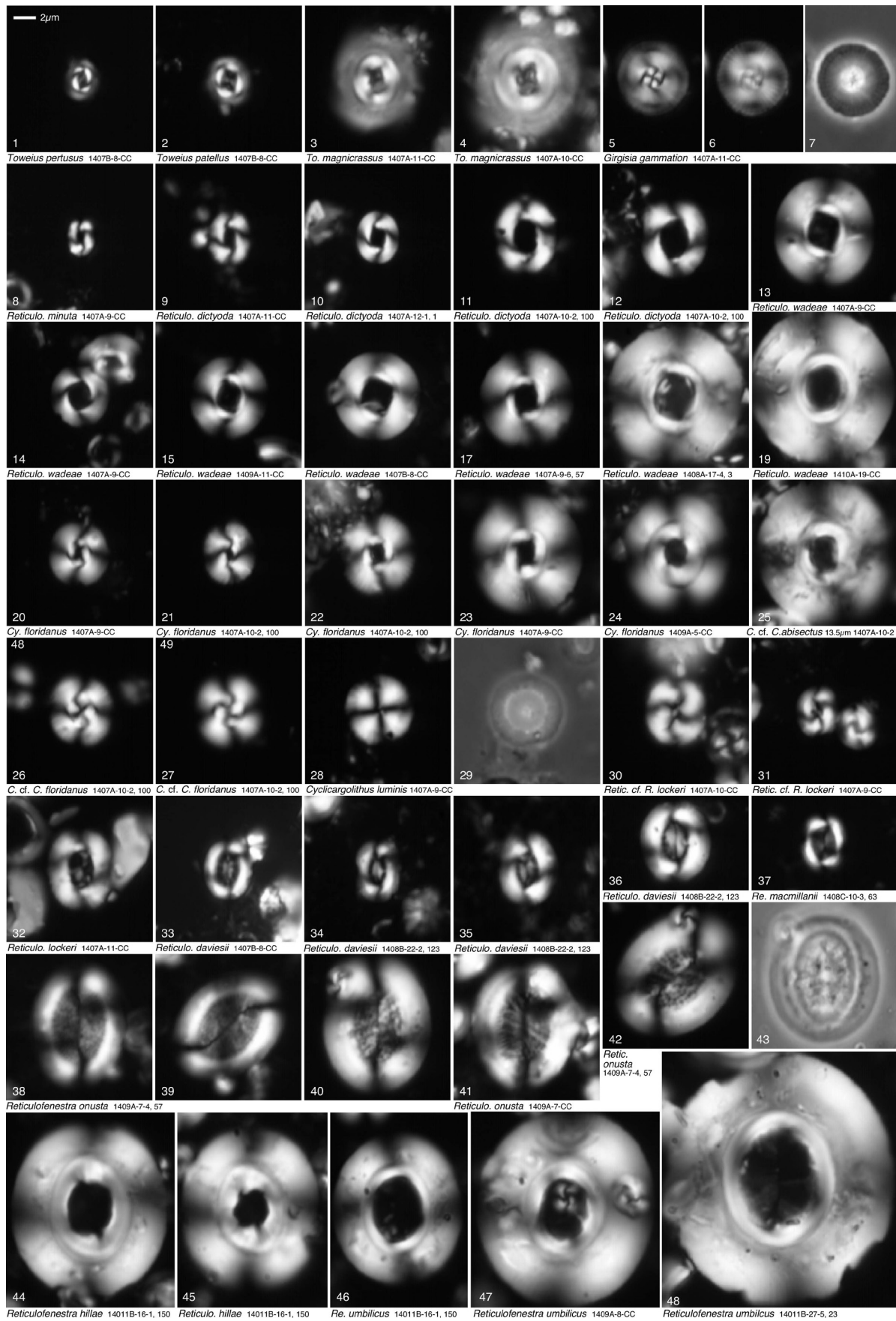


## Plate 2

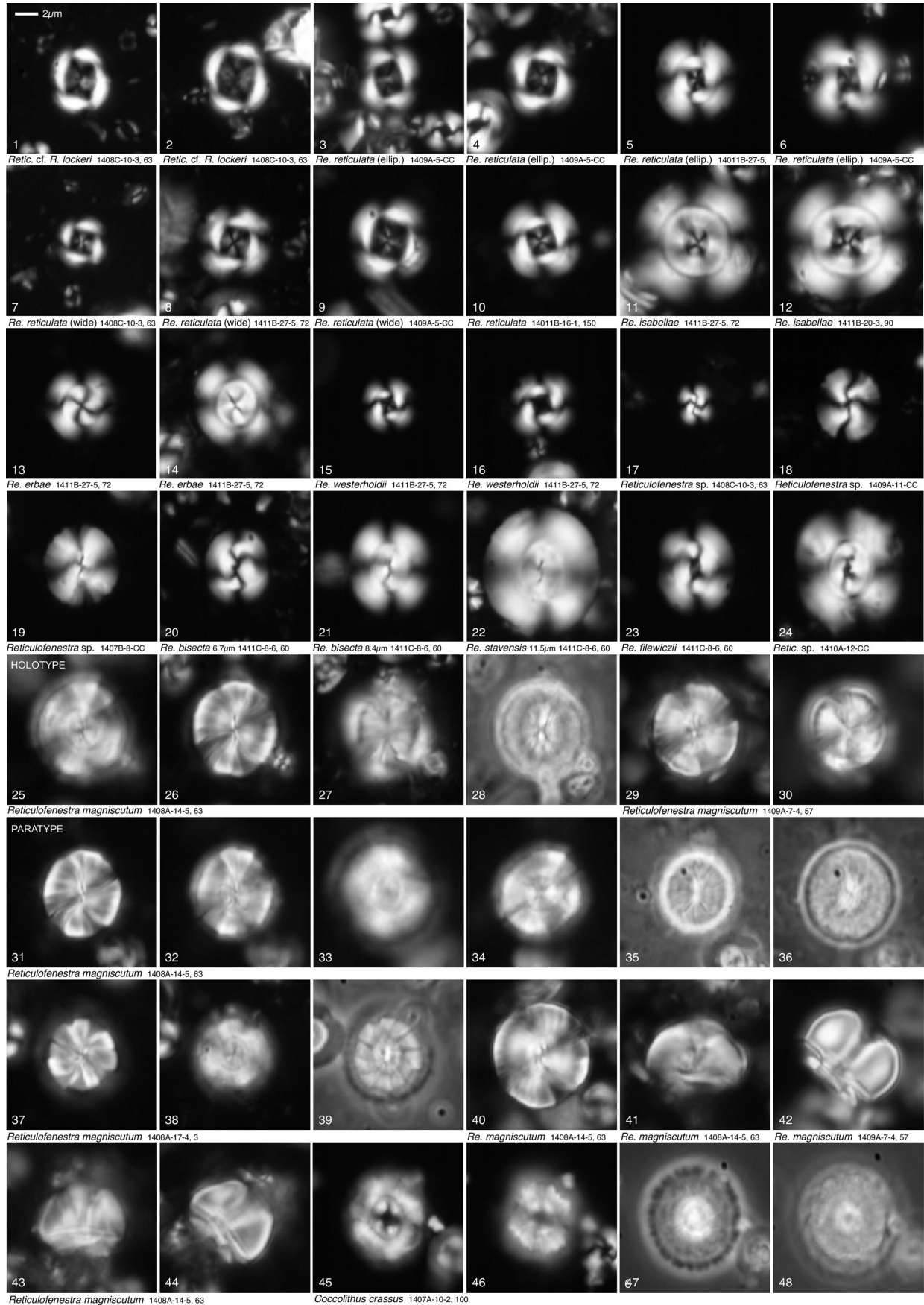


## Plate 3

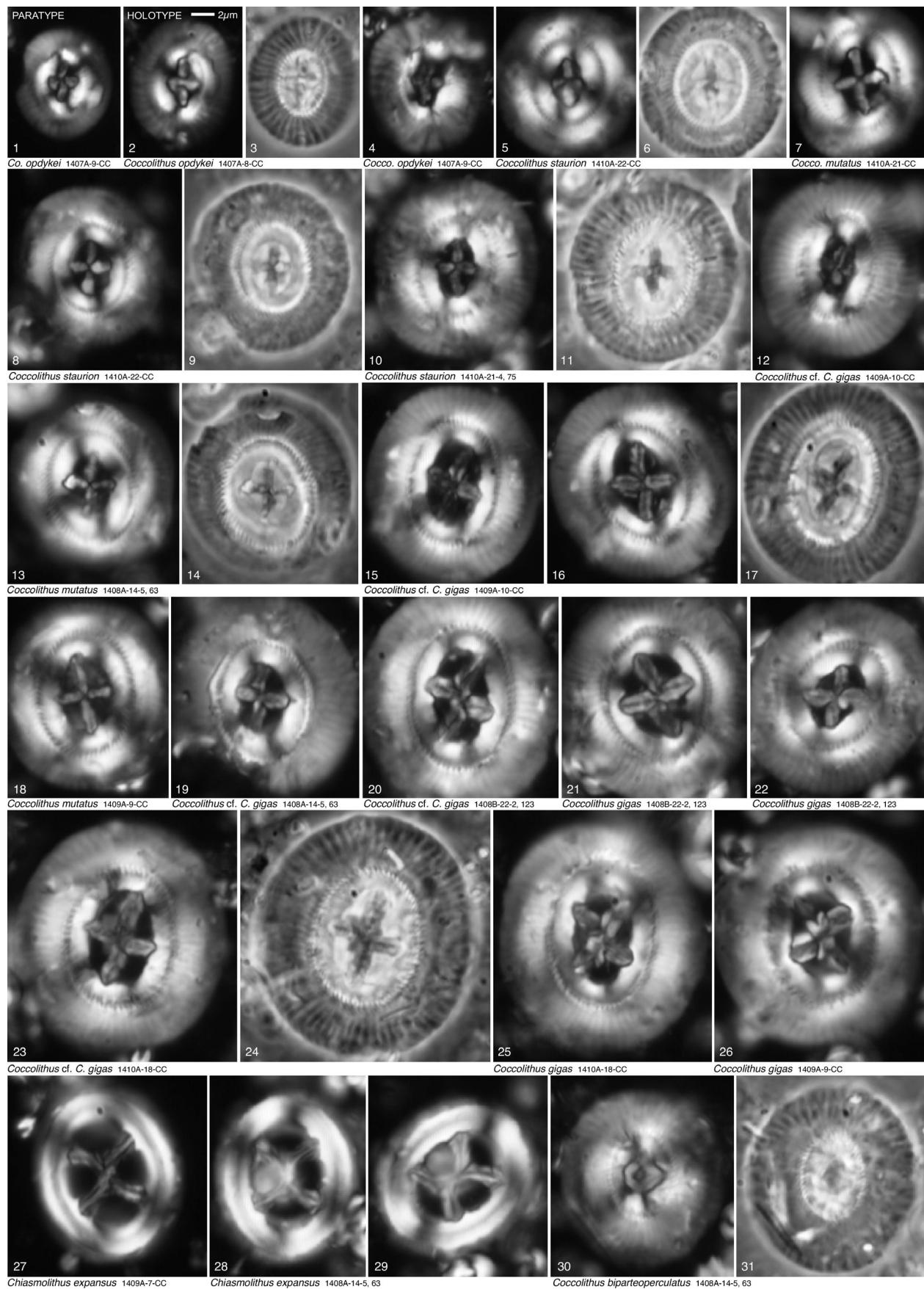


## Plate 4

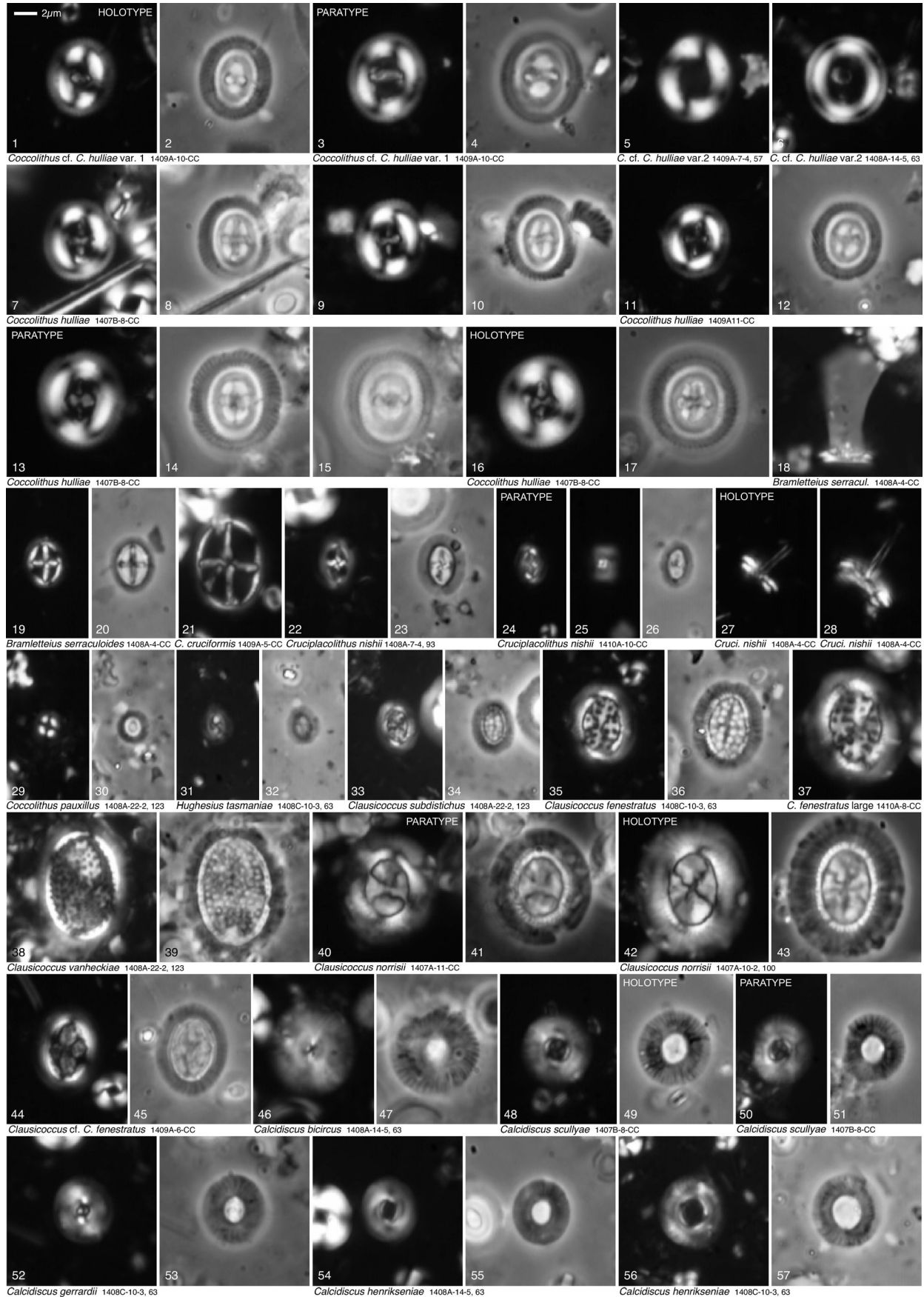


## Plate 5

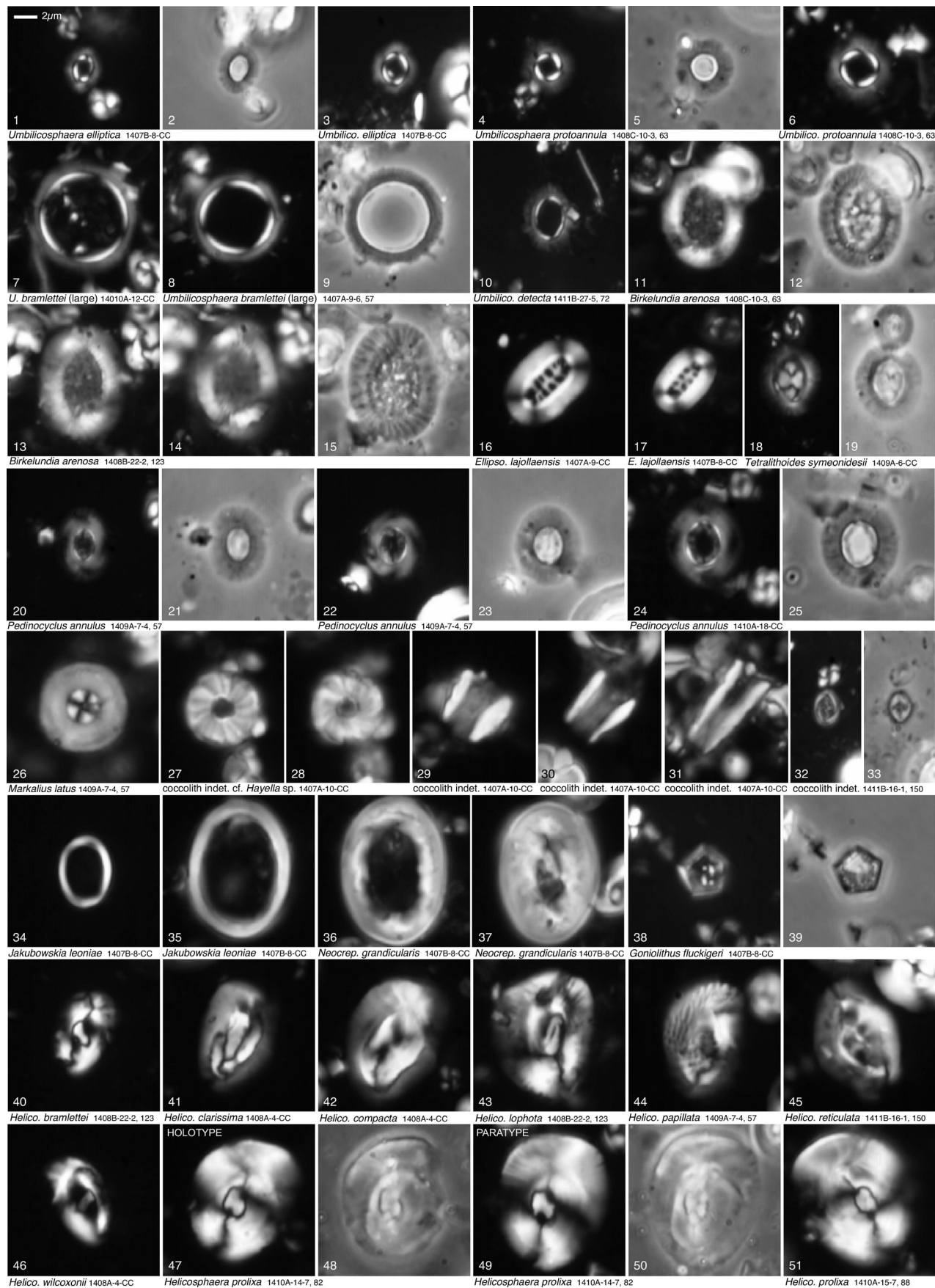


## Plate 6

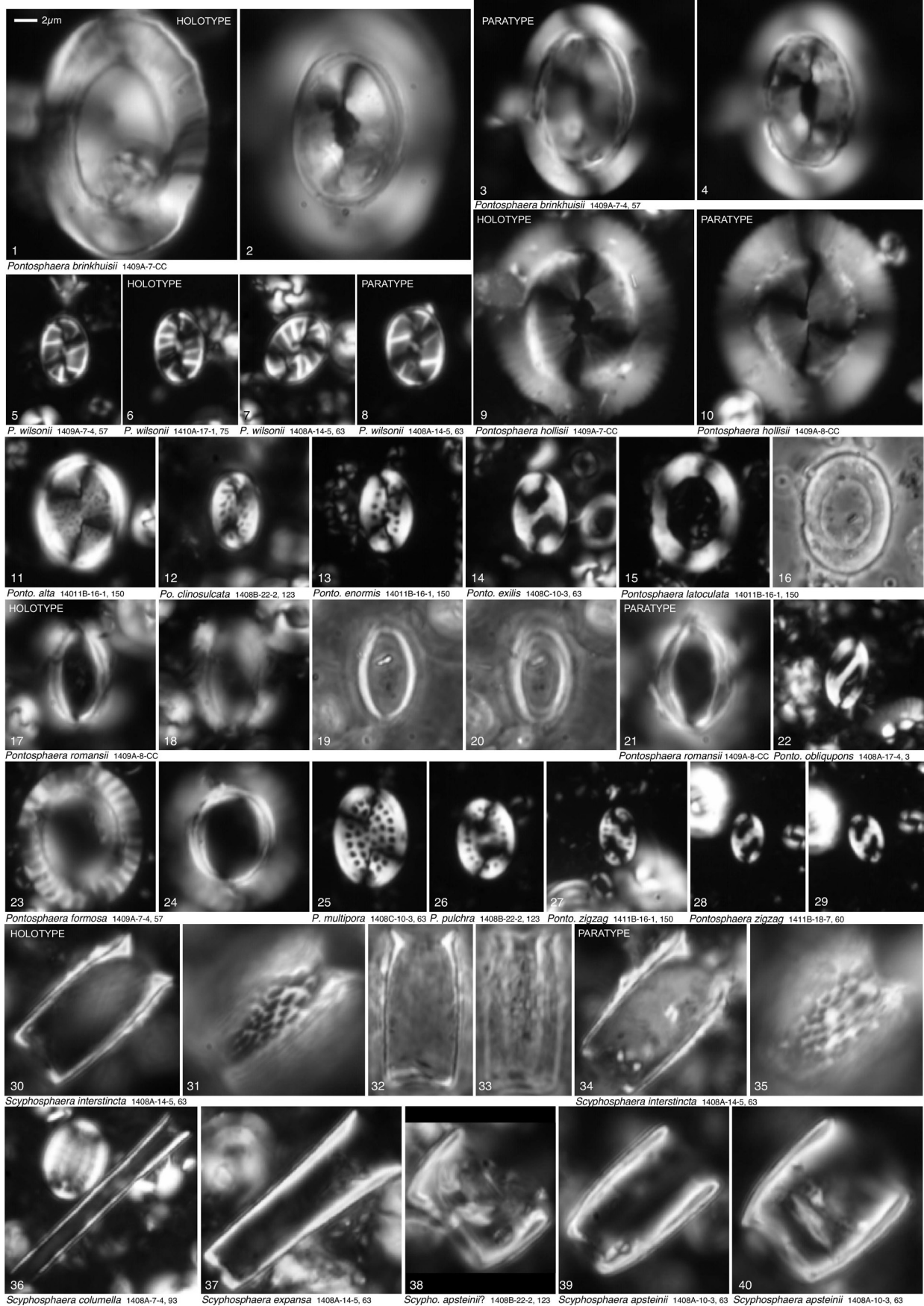


## Plate 7

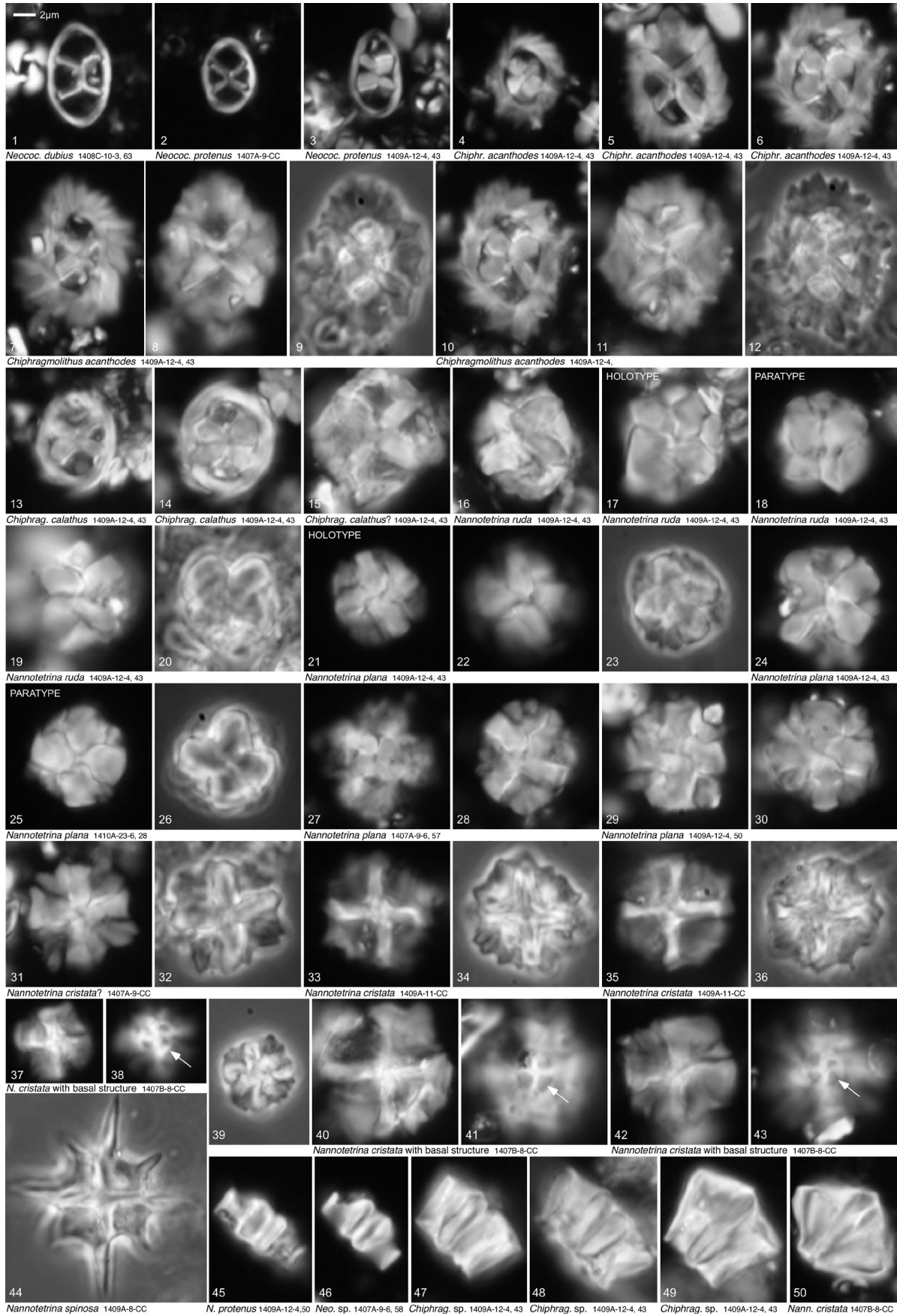


## Plate 8

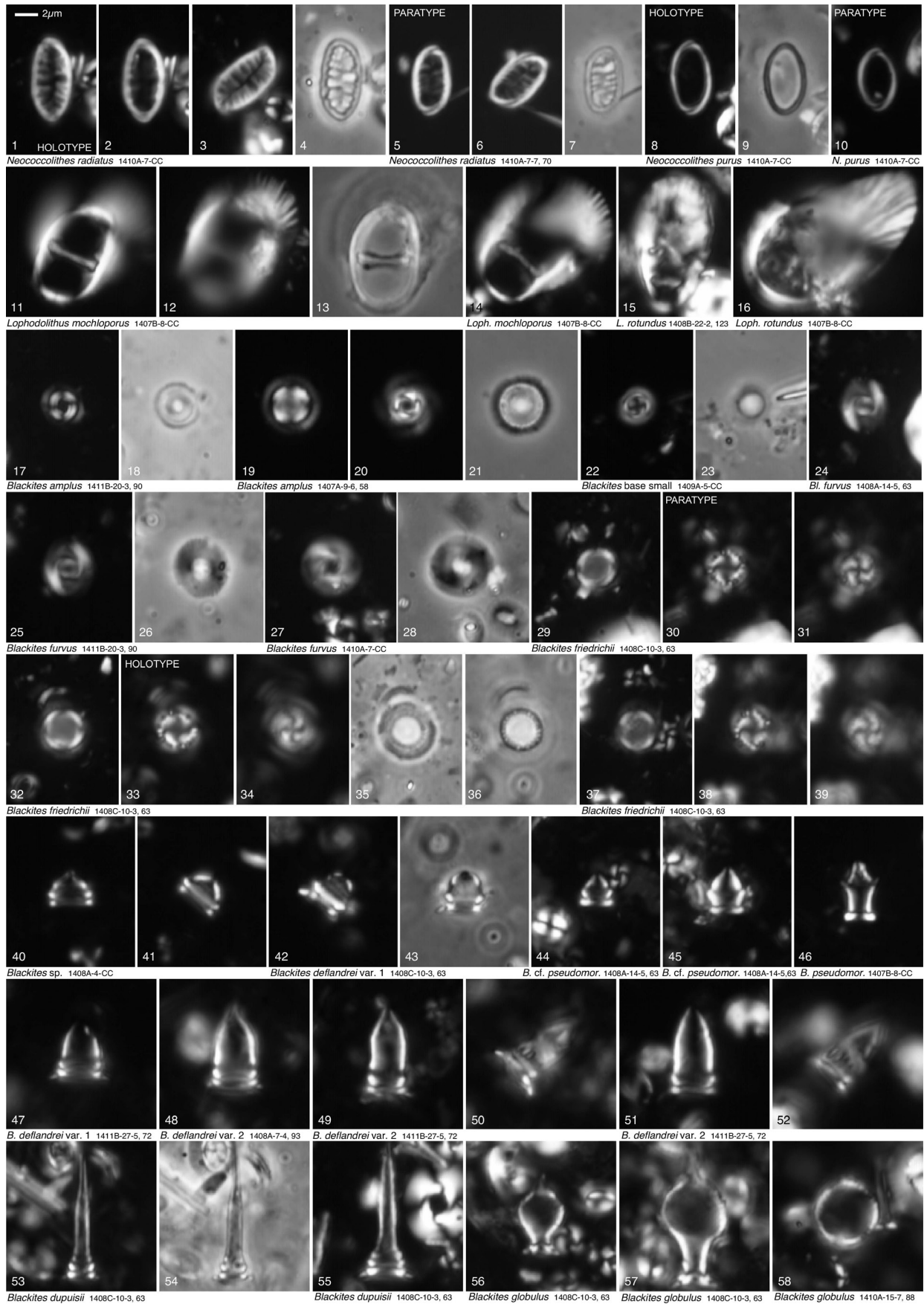


## Plate 9

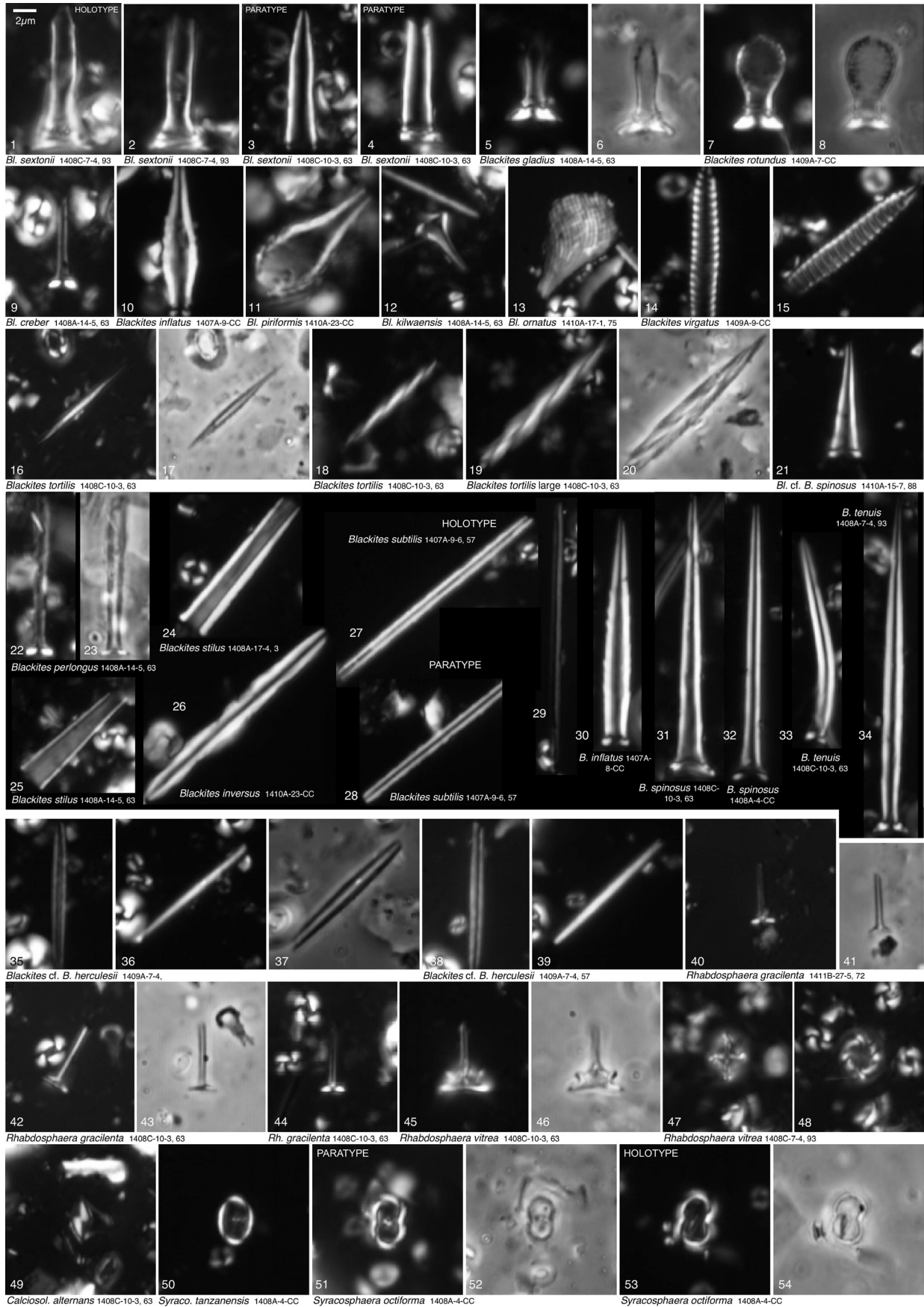


## Plate 10

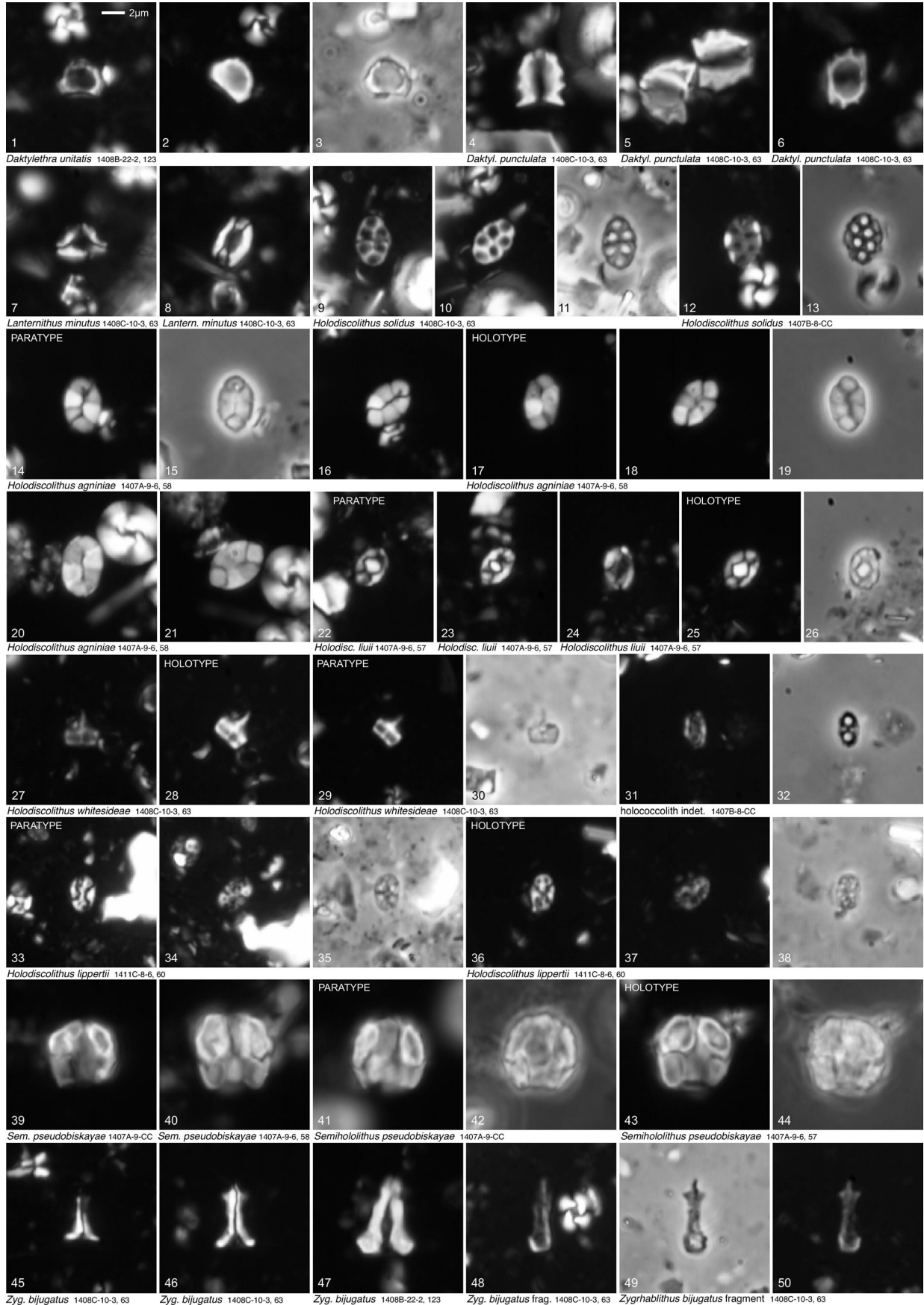


## Plate 11

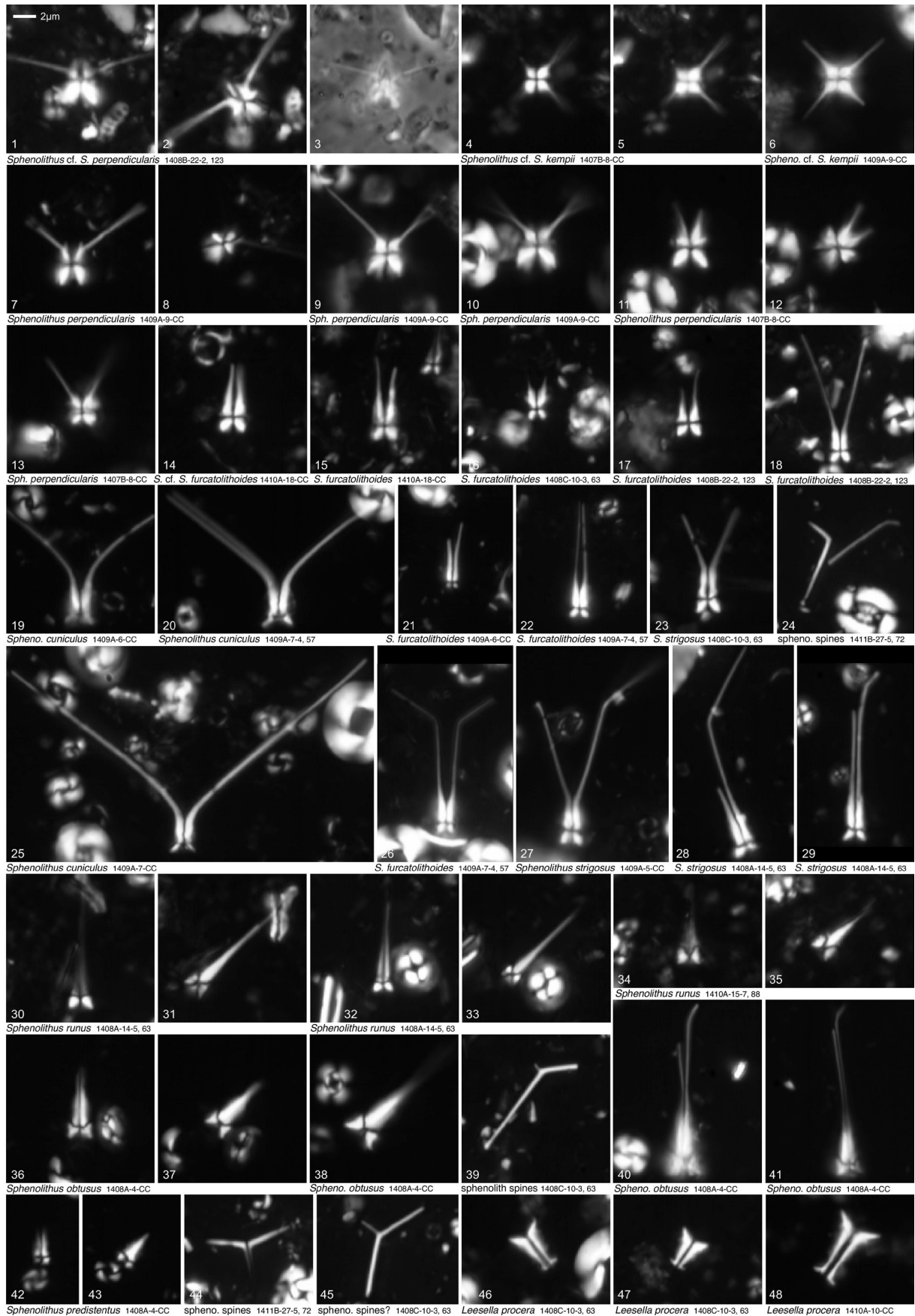


## Plate 12

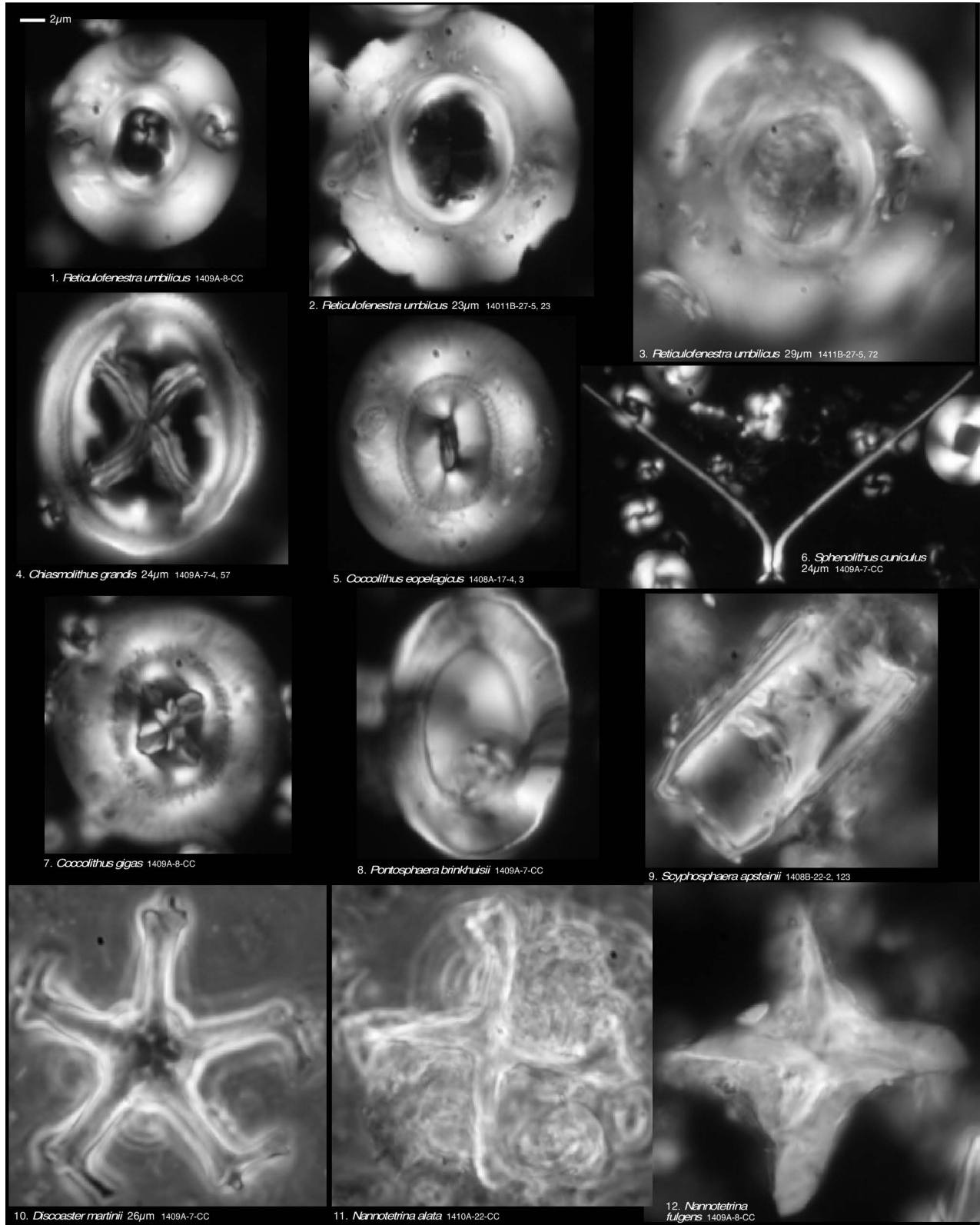


## Plate 13

scale bars are 2µm

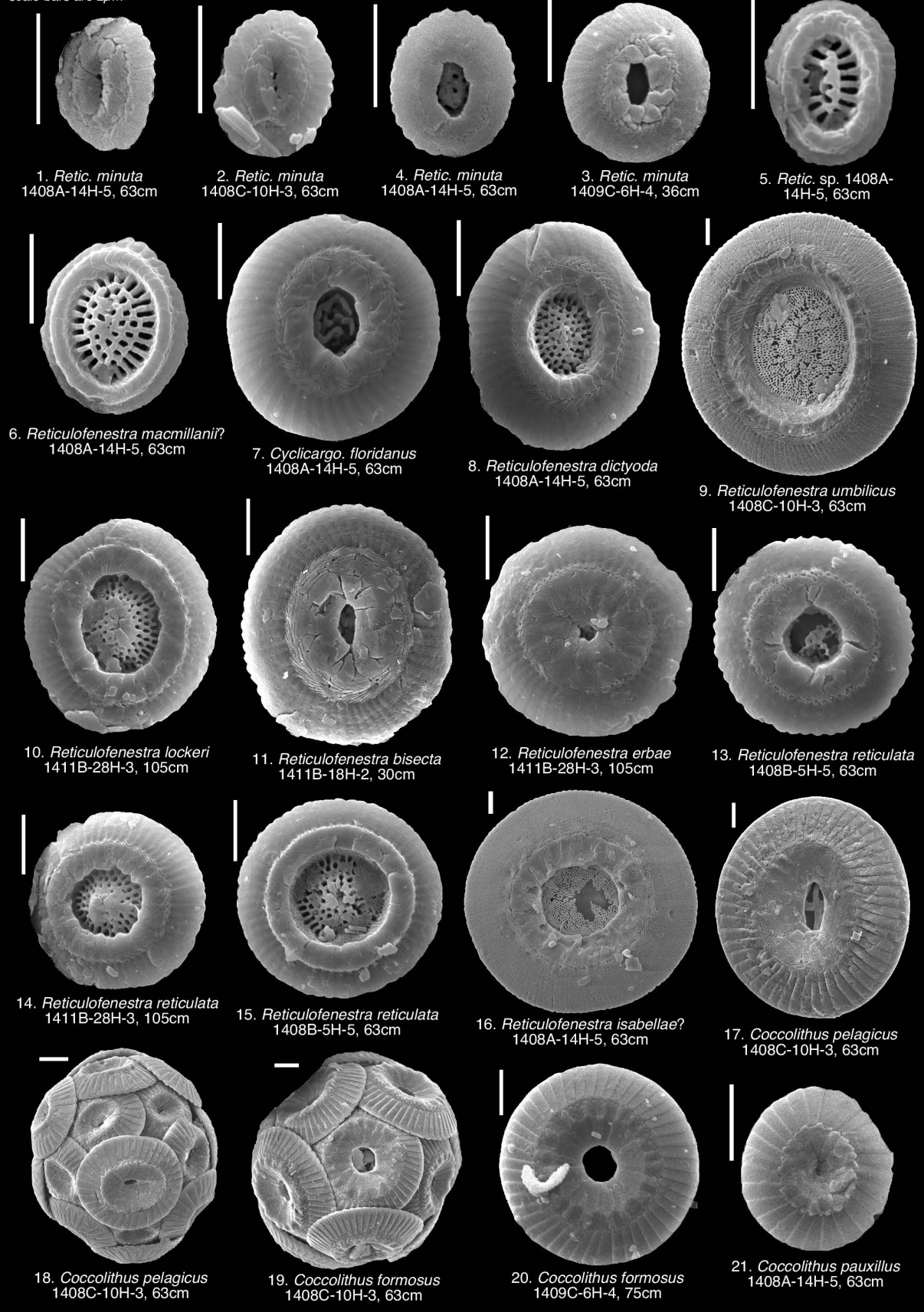


## Plate 14

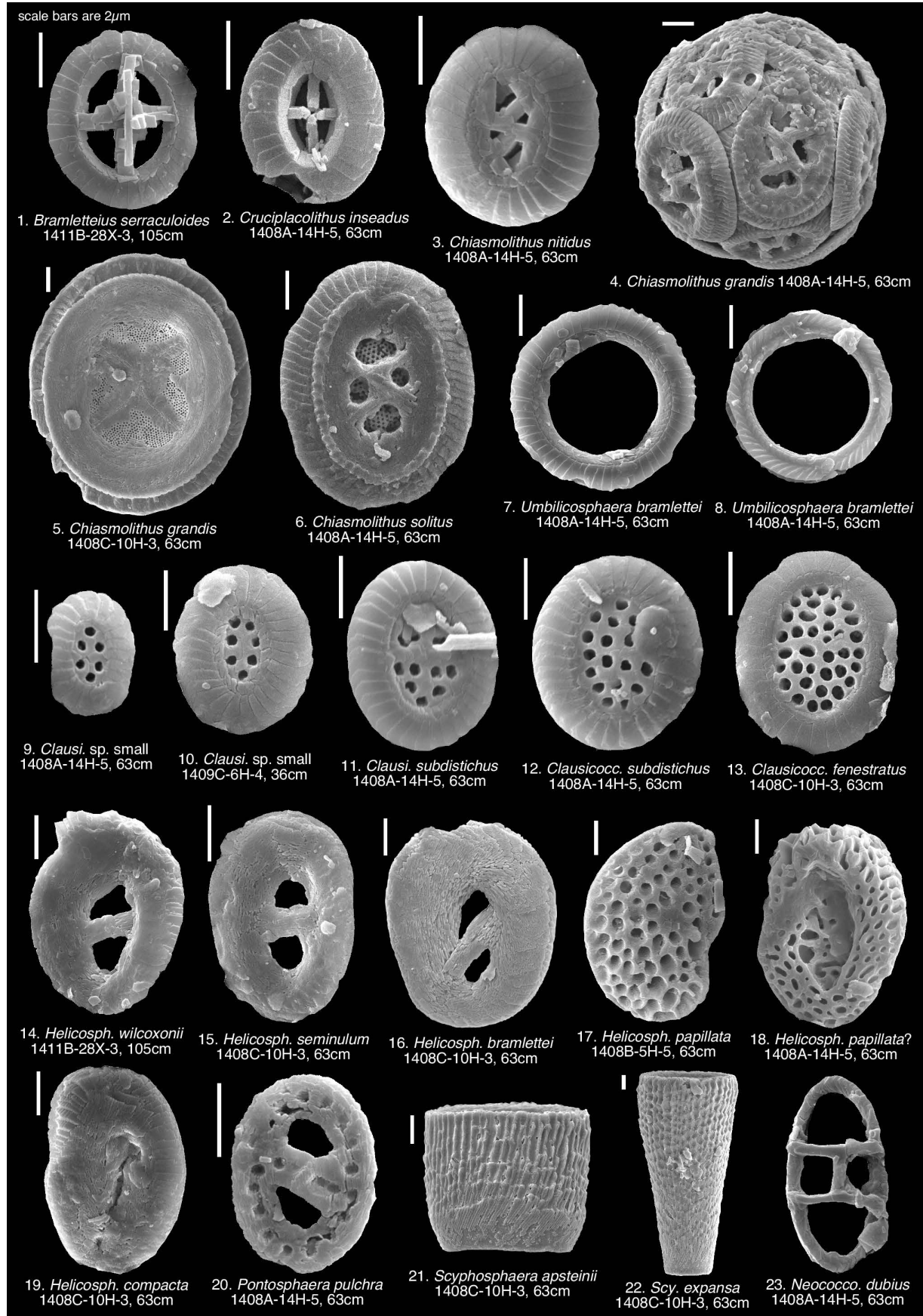
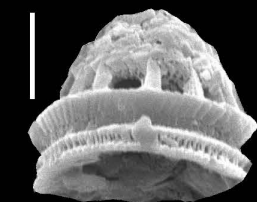
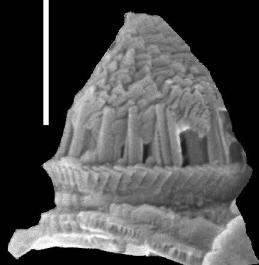


## Plate 15

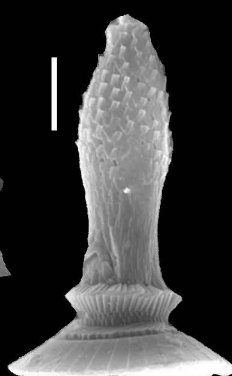
scale bars are 2µm



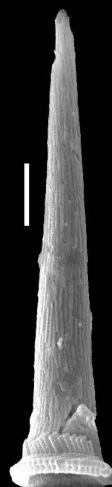
1. *Blackites deflandrei* var. 1  
1408B-5H-5, 63cm



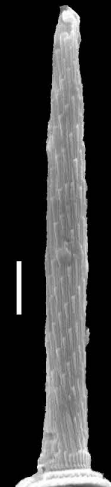
2. *Blackites deflandrei* var. 1  
1408C-7H-4, 93cm



3. *Blackites gladius*  
1408A-14H-5, 63cm



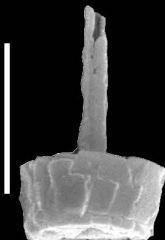
4. *B. spinosus*  
1408A-22X-2, 63cm



5. *B. tenuis* 1408A-14H-5, 63cm



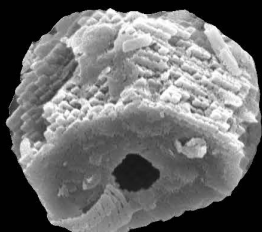
6. *B. tortilis*  
1408A-14H-5, 63cm



7. *Pocillithus spinulifer*  
1408A-14H-5, 63cm



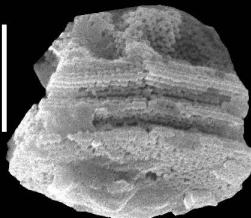
8. *Pocillithus spinulifer?* 1408A-14H-5, 63cm



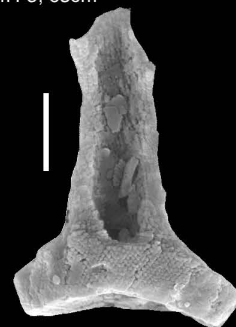
9. *Daktylethra unitatis* 1408B-5H-5, 63cm



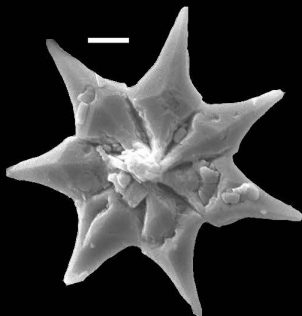
10. *Holodiscolithus solidus*  
1408C-10H-5, 63cm



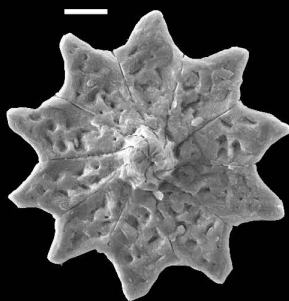
11. *Lanternithus minutus*  
1408C-10H-5, 63cm



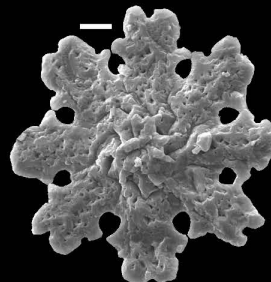
12. *Z. bijugatus* 1411B-28X-3, 105



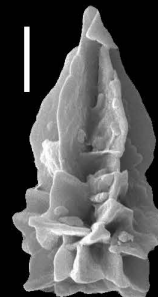
13. *Discoaster saipanensis*  
1409C-6H-4, 75cm



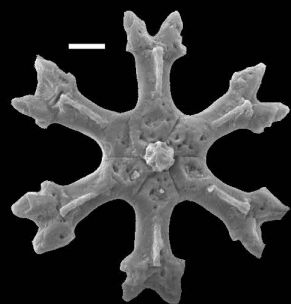
14. *Discoaster barbadiensis*  
1408C-10H-3, 63cm



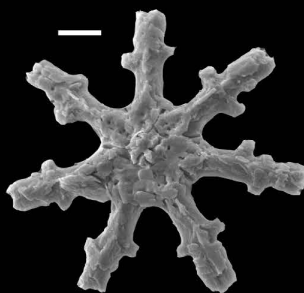
15. *Discoaster* cf. *D. nodifer*  
1408A-14H-5, 63cm



16. *Sphenolithus radians*  
1409C-6H-4, 75cm



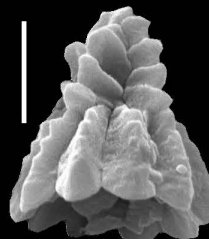
17. *Discoaster distinctus*  
1408C-10H-3, 63cm



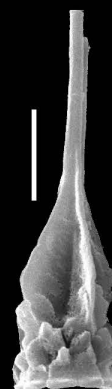
18. *Discoaster nodifer* 1408C-10H-3, 63cm



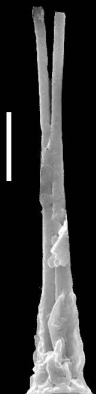
19. *Sphenolithus moriformis*  
1408A-14H-5, 63cm



20. *Sph. spiniger*  
1409C-6H-4, 75cm



21. *Sph. obtusus*  
1408B-5H-5, 63cm



22. *Sph. strigosus*  
1408A-14H-5